Osteogenic and Chondrogenic Differentiation of rBMSCs on Microsphere-Based Scaffolds Sintered Using Subcritical CO_2

By

Manjari Bhamidipati

Submitted to the graduate degree program in Bioengineering and the Graduate Faculty of the University of Kansas in partial fulfillment of the requirements for the degree of Master of Science.

_____

Chairperson, Dr. Michael Detamore

_____

Dr. Stevin Gehrke

_____

Dr. Aaron Scurto

Date Defended: November 11, 2011

The Thesis Committee for Manjari Bhamidipati

certifies that this is the approved version of the following thesis:

Osteogenic and Chondrogenic Differentiation of rBMSCs on Microsphere-Based Scaffolds Sintered Using Subcritical CO_2

_____

Chairperson, Dr. Michael Detamore

Date approved: November 29, 2011

Abstract

Large bone defects remain a major clinical orthopedic challenge. It has been predicted that osteoarthritis will affect over 100 million adults in the United States by the year 2030.(1) Current treatments for repairing bone defects include the use of bone grafts (autologous and allogenic) or implants (polymeric or metallic). These approaches have significant limitations due to insufficient supply, potential disease transmission, rejection, cost and the inability to integrate with the surrounding host tissue.(1)

The engineering of bone and cartilage tissue offers new therapeutic strategies to treat bone defects. Several scaffold-based approaches have been used in the past. However, this thesis presents a novel microsphere-based scaffold approach, sintered using subcritical carbon dioxide for osteogenic and chondrogenic tissue regeneration.

As a next step in the fabrication of three-dimensional tissue engineered scaffolds, this thesis primarily focused on subcritical carbon dioxide sintering for forming scaffolds, performance of these scaffolds in culture for 6 weeks, and evaluation of two different polymers in osteogenic and chondrogenic differentiation.

In this investigation, both temperature and pressure (along with time) were necessary to control during the CO_2 sintering of PCL (higher temperature and pressure conditions with longer exposure time), as opposed to PLGA, which was sintered at ambient temperature and pressure conditions (for 1 hour exposure). The results obtained showed the feasibility of using these constructs for bone and cartilage tissue regeneration. Biochemical analysis, gene expression and

histological staining were used to analyze the data. The mechanical integrity of the constructs was evaluated at the beginning and end of the culture period. The onset of PLGA degradation for the CO_2 sintered microspheres in this study appeared at 1.5 weeks which affected chondrogenesis. With osteogenesis, the Osteogenic PLGA group showed greater calcium content value over the Osteogenic PCL group while PCL retained its shape, size and mechanical integrity and had twice as many cells per construct at 6 weeks.

In conclusion, this thesis lays a foundation to explore numerous applications using subcritical carbon dioxide sintering for tissue engineering applications.

Acknowledgments

I thank my advisor Dr. Michael Detamore for all his time, support, guidance and constant encouragement during my Masters. I would like to thank my committee members Drs. Stevin Gehrke and Aaron Scurto for all their valuable time and suggestions.

I thank my parents, Prameela and Madhava Rao, sister Madhuri and brother-in-law Ram for all the love, support and advice. I thank my boyfriend Sunil, for always being there and encouraging me.

I thank all my lab members especially our post docs Ju and Neethu and our lab manager Peggy for all their help, suggestions, exchange of ideas and all the fun times in the lab.

This work was supported by NIH grant number R21 EB007313.

Table of Contents

List of Figures

List of Tables

Chapter 1 Introduction

The overall objective of this thesis was to characterize a novel microsphere-based scaffold sintered using dense phase subcritical carbon dioxide for osteogenic (bone) and chondrogenic (cartilage) tissue regeneration. To achieve this objective, dense phase carbon dioxide sintering of two polymer microspheres poly(lactide-co-glycolide) (PLGA) or poly(caprolactone) (PCL), was carried out to produce shape-specific scaffolds that would enable cell attachment and proliferation. The primary challenge of this thesis was to identify appropriate sintering conditions for PCL. The next step was to evaluate the *in vitro* performance of these two polymers for differentiation into osteogenic tissue and evaluate the performance of PLGA for differentiation into chondrogenic tissue and then have a detailed look at the bioactivity and tissue growth. Rat bone marrow mesenchymal stromal cells (rBMSCs) were used to evaluate the differentiation into osteogenic and chondrogenic tissues. Differentiation of rBMSCs was characterized according to biochemical content and histological staining. Gene expression was quantified via RT-PCR. Additionally, the mechanical integrity of the constructs was tested.

To achieve the overall objective, two specific aims were designed: (1) to fabricate a novel dense phase CO_2 sintered PLGA and PCL microsphere based scaffold, and (2) evaluate *in vitro* performance of PLGA and PCL scaffolds in osteogenic and chondrogenic differentiation of rat bone marrow mesenchymal stromal cells (rBMSCs).

The organization of the remaining chapters is as follows:

Chapter 2 serves to provide background information in which the literature pertinent to subsequent chapters is reviewed. Also provided in Chapter 2 is a discussion of applications of carbon dioxide (CO_2) technology in the field of tissue engineering, various scaffold fabrication methods making use of CO_2 technology, encapsulation of growth factors and mammalian cells using CO_2 and various factors effecting the porosity in scaffolds prepared using CO_2 technology and its effect on tissue growth.

After the background information is established in Chapter 2, Chapters 3 addresses the experiments performed to satisfy the aforementioned specific aims. The deliverables included osteogenic and chondrogenic gene expression, biochemical output, tissue synthesis, and mechanical properties of constructs cultured with rat bone marrow mesenchymal stromal cells (rBMSCs).

Chapter 4 contains the conclusion. Findings from all experiments are summarized in a global context and future research directions are discussed.

Chapter 2 The Future of Carbon Dioxide for Polymer Processing in Tissue Engineering

2.1 Abstract

The use of CO_2 for scaffold fabrication in tissue engineering was popularized in the mid-1990s as a tool for foaming polymer scaffolds, but had fallen out of favor to some extent due to challenges with pore interconnectivity. However, the issue of pore interconnectivity has been addressed by virtue of merging pores by creating extremely high porosities. In addition to CO_2 foaming, several groups have leveraged CO_2 as a swelling agent to impregnate scaffolds with drugs and other bioactive additives, and for encapsulation of plasmids within scaffolds for gene delivery. Moreover, in contrast to CO_2 foaming, which typically relies on supercritical CO_2 at very high pressures, CO_2 at much lower pressures has also been used to sinter polymeric microspheres together in the presence of cells to create cell-seeded scaffolds in a single step. CO_2 has a number of advantages for polymer processing in tissue engineering, including its ease of use, low cost, and the opportunity to circumvent the use of organic solvents. With its numerous advantages, and the continuing diversification of its uses, a resurgence in the application of CO_2 in tissue engineering is being witnessed.

2.2 Introduction:

Carbon dioxide has found enormous uses in virtually all fields of science and research over the past several decades. Its use as a supercritical fluid, along with its plasticizing and solvent properties have enabled it to be used in a wide variety of tissue engineering and regenerative medicine applications.(2) In the field of tissue engineering, scaffolds provide a platform for cell attachment and proliferation, which can be achieved with the 3D biomaterial having a high porosity and high pore interconnectivity.(3) The presence of pores in the scaffold enables nutrient and oxygen transport, waste removal, and helps in the growth and proliferation of the cells. The majority of current processing techniques for scaffold fabrication use organic solvents and/or high temperatures.(3) Carbon dioxide technology provides an alternative to these methods with many applications described in the literature.(4)

Colton and Suh (5) in 1987 reported one of the first use of CO_2 and N_2 to produce foams of polystyrene. The first mention of CO_2 foams for tissue engineering scaffolds can be found in a 1991 patent,(6) a technique that was first brought to the tissue engineering literature by Mooney *et al.* (7) in 1996, who made porous disks of poly (D, L-lactic-co-glycolic acid) by exposure to CO_2 for prolonged periods of time. While porosities up to 93% were obtained, there was only partial interconnectivity between the pores. They also observed the presence of a non-porous skin layer, which turned out to be a major challenge to overcome for other groups that followed as well.

The use of supercritical CO_2 for generating porous polymeric foams has generated significant interest over the years. Several advancements have been made in the tissue

engineering field since its first use by Mooney *et al.*(7) Most of the techniques utilizing supercritical fluid technology in pharmaceutical and drug delivery applications have been reviewed eloquently and thoroughly by Howdle and Shakesheff.(8) Hence, this review will not attempt to address previously reviewed methods, and will focus instead on recent developments in tissue engineering applications. The processing conditions developed for improving porosity and pore interconnectivity in these three-dimensional constructs will also be discussed. The impetus for this review is that with the rapid growth in the number of advanced biomaterials and fabrication methods for scaffolds in tissue engineering, the field has largely moved away from CO_2 in fabrication methods, but there are a number of advantages and opportunities with CO_2 of which many investigators are not aware. CO_2 processing is relatively straightforward and affordable to incorporate in a laboratory, and we encourage both industry and academia to take another look at what CO_2 may add to their particular application.

2.3 Properties of Carbon Dioxide

A supercritical fluid is a dense phase fluid whose pressure and temperature are above its critical point. At the critical point of a substance, a single phase occurs that has liquid-like density and gas-like viscosity and compressibility.(9) It is important to note that above the critical temperature, compression yields a continuous increase in fluid density without condensation to a liquid state. These properties can be easily tuned by changes in pressure and temperature. Supercritical fluid and dense-phase gas (near-critical) technology is an area of intense fundamental and applied research, especially as an environmentally-benign solvent

alternative. Carbon dioxide is the most often used substance, in part because it has a low critical temperature and pressure (T_c=31.1 ˚C and P_c=73.8 bar), as seen in Figure 1, which makes it suitable for processing thermo-sensitive compounds. Furthermore, it has the additional advantages of being inexpensive, non-toxic and non-flammable. The recovery of final products and removal of CO_2 can be done easily with no residue left behind.(10)

CO_2 helps in reducing the polymer melt viscosity (11-15) by decreasing the glass transition temperature (T_g) or melting temperature (T_m) due to its high solubility in polymers.(16) The molecular structure and morphology of polymers greatly influence CO_2 solubility and diffusivity.(8) The carbonyl or ether groups in the backbone or on side chains of a polymer interact with CO_2 and help with the dissolution of CO_2 within the polymer. Polymers that have ether groups in their backbone structure such as poly(ethylene glycol) (PEG) have been shown to have stronger interactions with CO_2 than polyesters, which have ester functional groups in their main chains. This has been attributed to weak Lewis acid-base interactions between them.(17) Steric hindrance can also influence solubility of CO_2 in the polymer. In the case of poly(lactic acid) (PLA) and poly(lactic-co-glycolic acid) (PLGA), both polymers have the same chemical structure in their main chains, but the solubility of CO_2 is higher in PLA than in PLGA. PLGA co-polymers that have high lactic acid content also have fewer methyl groups, which enable them to have less hindrance during their interaction with CO_2. The accessible free volume caused by methyl pendant groups also improves solubility. Therefore, with increasing glycolic acid content in PLGA copolymers, the solubility of CO_2 decreases.(18) Also, for highly crystalline polymers like PLA (98:2, 20% crystallinity), PGA, PEG and PCL, CO_2 has a relatively low solubility and it cannot easily diffuse at temperatures below their melting points. Amorphous

poly(DL-lactic acid) ($P_{DL}LA$) and PLGA allow CO_2 to diffuse more easily due to the presence of a large free volume within their structures.(19)

All of these properties have widely enabled CO_2 to be used in the field of tissue engineering for various applications such as in the production of polymer scaffolds and composites, encapsulation and release of bioactive compounds, and encapsulation of mammalian cells.(8)

2.4 Preparation of 3D Scaffolds in Tissue Engineering

Porous three-dimensional scaffolds used in tissue engineering, help with cell attachment, differentiation and proliferation to regenerate a given tissue of interest.(20-22) Particularly for musculoskeletal tissues, the biodegradable constructs must have adequate mechanical integrity to support the cells and the load bearing activities of the tissue. They may also benefit from having appropriate physico-chemical properties to release a bioactive compound that would help guide the cells in integrating with the surrounding tissue.(23) To date, several methods have been reported in the literature for the preparation of 3D scaffolds, some of which include processes such as solvent casting with particulate leaching,(24) compression molding,(25) freeze drying,(26) heat sintering,(27, 28) injection molding,(29) layer-by-layer printing (30) or sintering (31) and electrospinning.(32) Each of these methods has its own advantages, but these methods typically make use of large amounts of organic solvents and/or exposure to elevated temperatures. Supercritical and dense-phase fluid technologies provide an attractive alternative to these traditional methods of scaffold fabrication. In this section, we discuss the strategies that

have been applied for creating three-dimensional porous polymer-based scaffolds and their applications from a tissue engineering perspective. Among several scaffold design parameters, a select few like pore size, porosity, and processing conditions are of high interest.

2.4.1 Gas foaming

Gas foaming is one of the most commonly used techniques making use of supercritical fluid technology for the fabrication of 3D scaffolds for tissue engineering. It was first described by de Ponti *et al.* in a 1991 patent where gas foaming was used for making scaffolds with closed pore structures from biodegradable poly(α-hydroxyacids) like P_LLA, $P_{DL}LA$, PGA and PLGA (Figure 2).(33) In this technique, the polymer is saturated with CO_2, which at high pressures causes it to plasticize by reducing the glass transition temperature. This reduction in T_g of the polymer is achieved as a result of the intermolecular interactions between CO_2 and the polymer. Greater T_g depression is observed in polymers that have stronger interactions. Following saturation of the polymer with CO_2, rapid depressurization causes thermodynamic instability and results in the formation of nucleated gas cells that give rise to pores within the scaffold. This technique is mainly applicable for amorphous and semi-crystalline polymers that have a higher affinity for CO_2 when compared to crystalline polymers.(10) Mooney *et al.*(7) popularized this process by making porous poly(D, L-lactic-co-glycolic acid) disks by exposure to CO_2 for 3 days followed by rapid depressurization, which resulted in gas nucleation and formation of pores up to 97%. However, this process also formed a non-porous skin layer over the entire surface of the polymer matrix, which is not suitable for cell adhesion.(7) To overcome this issue, Mooney and his co-workers (34) introduced salt (NaCl) particles to the polymer solution prior to gas foaming. Leaching of this porogen following fabrication of the polymer foam created an interconnected

open pore network. The degree of porosity and interconnectivity was regulated by altering the salt/polymer ratio and the salt particle size. They found that the polymer disks containing a large percentage (95%) of large NaCl particles did not have an external, nonporous skin over the scaffold surface.(34) Several improvements to the conventional gas foaming technique have been made over the last few years, enabling it to be used for various applications. Barry *et al.*(35) used the gas foaming method to create poly(ethyl methacrylate)/tetrahydrofurfuryl methacrylate (PEMA/THFMA) foams that were found to have about 87% porosity with nearly 57% open pores. These foams supported bovine chondrocyte proliferation by displaying increased glycosaminoglycan synthesis and retention of rounded cell morphology.

Salerno *et al.*(36) combined gas foaming with microparticulate templating to achieve open pore biodegradable foams made of PCL with a controlled porous architecture. Composites of PCL were combined with micrometric NaCl particles in concentrations ranging from 70/30 to 20/80 wt% at 70 ºC for 3 hrs at a pressure of 65 bar. It was observed that porosity, pore size and pore interconnectivity was controlled by optimizing the processing parameters. Spatial gradients of pore size and porosity were achieved within the same scaffold by using a microparticle concentration gradient of NaCl. Gualandi *et al.*(37) prepared polymeric foams of ω-pentadecalactone (PDL) and ε-caprolactone (CL) (poly(PDL-CL)) using supercritical CO_2 foaming. They observed that foaming was possible at a temperature greater than the melting temperature of the co-polymer. The pore diameter and porosity were found to be dependent on the cooling rate. A cooling rate of 0.23 ºC/min resulted in a pore diameter of 225 μm with 70% porosity. Variations in pore size and interconnectivity were achieved by altering the rate of depressurization. Further details about the processing conditions have been listed in Table 1.

Mathieu *et al.*(38) applied supercritical CO_2 gas foaming technology to produce composite cellular structures having a heterogeneous architecture of pores in PLA foams containing hydroxyapatite (HA). They observed that addition of HA resulted in more heterogeneous foams than with β-tricalcium phosphate (β-TCP). Ceramic particles of HA and β-TCP were distributed in the pore walls of the composite foams, thereby providing an efficient reinforcement of the matrix. These foams had an average pore size from 200 to 400 μm with porosities between 78% and 92%. Tsivintzelis *et al.*(39) found that crystalline polymers such as PCL can undergo supercritical CO_2 foaming with the addition of small amounts of organic solvents such as ethanol. Addition of ethanol resulted in more uniform cell structures in the scaffolds than those prepared using CO_2 alone, and also resulted in larger pore formation. However, all of the samples had a dense unfoamed skin usually apparent with the gas foaming technique.

Gas foaming can produce open-cell, interconnected pores in a solvent-free process under the right conditions. However, the greater degree of porosity can have an effect on the mechanical integrity of the construct. White *et al.*(40) addressed this issue of optimizing porosity and mechanical strength. They formed foams made of different molecular weights of poly(DL-lactic acid) ($P_{DL}LA$) (57, 25 and 15 kDa) and varied the depressurization rate. During depressurization, super-saturation of CO_2 occurred within the polymer, which led to nucleated bubble formation. It was observed that the rapid depressurization rate produced scaffolds with homogeneous pore distributions with closed pores. A decrease in depressurization rates resulted in wider pore distributions in the scaffolds with larger, interconnected pores. Compressive testing of these constructs showed that the higher MW $P_{DL}LA$ (52 kDa) showed elastomeric properties

(a linear elastic region, a collapse plateau region and a densification region), while the lower MW $P_{DL}LA$ (25 and 15 kDa) was more brittle in nature. The 52 kDa $P_{DL}LA$ showed potential for bone tissue engineering applications. Further details about improvements in processing conditions have been described briefly in Table 1.

Gas foaming is one of the most commonly used techniques for making scaffolds using CO_2. With gas foaming, a variety of conditions and parameters have been investigated with different materials, and common concerns being pore interconnectivity and presence of a skin layer, which have been addressed with approaches such as salt leaching and use of high pressures with slow venting times.

2.4.2 Phase inversion

In the phase inversion method, a polymer solution is cast onto an inert support that is then immersed into a bath containing non-solvent for the polymer. Contact between the solvent and non-solvent results in a phase separation. Carbon dioxide is the most commonly used supercritical fluid that is being used as a non-solvent. Using CO_2 also avoids a drying step in the end, thereby resulting in a dry product free of all residual solvents. By tuning the process conditions such as pressure and temperature, the final structure of the product can be modified as needed.(4, 10) The phase inversion method using CO_2 as a non-solvent has been used successfully for the preparation of different polymeric scaffolds (Table 1).

Tsivintzelis *et al.*(41) used the phase inversion method to prepare PLLA foams. They observed that pore size decreased with pressure variation from 100-230 bar. Lesser initial polymer concentration led to the formation of larger pores. Reverchon *et al.*(42) also observed

that pore diameter decreased (from 15 to 7 μm) with increasing pressure (from 150 to 250 bar) for Poly(methyl methacrylate) (PMMA) foams. On the other hand, pore size increased from 8 to 12 μm on increasing the temperature from 35 to 65 ºC.

Duarte *et al.*(43) formed polymer matrices from starch and poly(L-lactic acid) (SPLA) by the phase inversion method. The resultant scaffolds had a porosity of 66% with macropores of 200 μm in diameter and micropores of 20-50 μm in diameter. These constructs had a 90% swelling and a weight loss of 25% after 21 days in culture. They later applied this method to form chitosan foams (44) with 29% porosity and an average pore size of 62 μm. Chitosan foams were found to be suitable for tissue engineering of bone and cartilage due to their physicochemical and biocompatibility.

Using supercritical fluid as a non-solvent during phase inversion helps in obtaining scaffolds that do not have any residual organic solvents. This approach has been used to form scaffolds from different polymeric materials and has found several applications.

2.4.3 Supercritical fluid emulsion templating

With the method of supercritical fluid emulsion templating, concentrated oil-in-water emulsions can be phase separated to create porous scaffolds. A variety of porous hydrophilic scaffolds can be prepared using this technique. The final porous product can be recovered by removing the internal phase, which is the emulsion. This technique has been extended to supercritical CO_2-in-water emulsions as well. Butler *et al.*(45) used this method to stabilize the C/W emulsions of acryl-amide polymers by using perfluoropolyether (PFPE) surfactants and poly(vinyl alcohol). Following polymerization, venting of CO_2 resulted in the formation of

interconnected pores within the polymer scaffold. They found that increasing the volume fraction of CO_2 internal phase increased porosity. It was also observed that by increasing the concentration of the surfactant, greater interconnectivity within the open pores could be achieved.(8) This method has been scarcely studied and there is potential for others to use this method if they want to obtain porous hydrophilic scaffolds.

2.4.4 Electrospinning

Electrospinning is an intriguing method that has been used for the production of polymeric fibers from biomaterials and composites.(46, 47) Here, an electric field is utilized to eject a charged polymer stream from a needle, which then results in the formation of micro-scale fibers under the influence of tangential stresses and bending instabilities.(46, 48) The diameter of the viscoelastic jet can be reduced to produce micron and nano-sized fibers by using the electrostatic repulsions between the surface charges.(49) Electrospinning has been used for a variety of applications in tissue engineering,(48) some of which include using electrospun scaffolds for cartilage replacement,(50-52) bone grafts,(53, 54) cardiac grafts.(55) They can also be used for seeding stem cells, (56, 57) and endothelial cells (58) to form a three-dimensional cellular network.

Supercritical CO_2 can be used as a swelling agent for polymers and can help impregnate the scaffolds with desirable additives such as drugs and bioactive compounds. Ayodeji *et al.*(48) embedded electrospun PCL with carboxytetramethylrhodamine using near critical CO_2 at a pressure of 3.44 MPa for a period of 2.5 hrs. They found that the individual fibers remained intact and showed a distinct non-woven fibrous network at a low temperature of 10 ˚C, but at a

higher temperature of 40 ˚C, the microstructure of the fibers began to change. They also observed a significant distribution of carboxytetramethylrhodamine throughout the surface of the PCL. Encapsulation of a bioactive molecule using supercritical CO_2 helps protect conformationally sensitive molecules from the shear forces present during the electrospinning process.(48)

Levit *et al.*(46) used supercritical CO_2 to produce poly(D,L-lactic acid) (PLA) electrospun fibers by using only electrostatic forces without the use of a liquid solvent. They found this new "supercritical fluid assisted electrospinning (SAES)" technique useful for producing large and small diameter fibers.

In 2010, Liu and colleagues (47) combined the traditional electrospinning process with a precipitation with a compressed fluid anti-solvent (PCA) method to produce micron and submicron sized polymeric fibers that had either a hollow or open-cell morphology. Supercritical CO_2 was used as the compressed fluid. Using this technique, they found that it was possible to obtain different fiber morphologies by simply adjusting the CO_2 pressure and that high temperature and pressures in excess of 100 bar were not needed. They also suggested using this technique to encapsulate live cells to produce celloidosome fibers.(47)

CO_2 offers the advantage of obtaining different diameter fibers with open pore structures without using a liquid solvent. It also helps in encapsulating live cells, heat-sensitive compounds within the electronspun fibers.

2.4.5 Hydrogel foaming using CO_2

Hydrogels are highly hydrated polymeric materials that consist of hydrophilic polymer chains. The cross-links between the polymer chains formed by various chemical bonds and physical interactions contribute to the structural integrity of the hydrogels.(59) Several studies have been reported in the literature that use high pressure CO_2 for the foaming of polymers to form hydrogels.

Tsioptsias *et al.*(60) investigated the extent and mechanism of supercritical CO_2 sorption by chitin hydrogels and the production of pores within these hydrogels. Chitin gels were prepared by dissolving chitin in a dimethylacetamide (DMA) and LiCl mixture followed by extensive washing in distilled water. Crosslinking within the gel was achieved by exposure to glutaraldehyde vapor at room temperature. They found that CO_2 sorption by the gel was due to its dissolution in the water of the hydrogel. Foaming of the hydrogel was observed during the depressurization, but it immediately shrunk on exposure to air. They found that freeze-drying the sample immediately after depressurization helped to retain the initial porous structure formed during the foaming process. However, a dense outer skin was present on the surface of the porous hydrogels.(60)

In 2010, Tsioptsias and others (61) proposed a mechanism for this hydrogel foaming technique. On depressurization, they proposed that there was heterogeneous nucleation at the polymer-water interface as well as homogeneous nucleation in the water phase, leading to the growth of pores. Following depressurization, temporary stabilization was achieved by cooling. Freeze-drying led to complete stabilization of the structure. In comparison, during polymer

foaming, there was only homogeneous nucleation in the polymer phase, which caused pore growth. Stabilization of the produced structure was achieved by vitrification.(61)

Annabi *et al.* (62) investigated the effect of supercritical CO_2 foaming on elastin-based hydrogels. Increasing the CO_2 pressure from 30 to 150 bar caused about a 60% increase in the hydrogel foaming ratio. It also accelerated the crosslinking time and facilitated coacervation leading to enormous changes in the macro and microstructures of the pores formed within the sample. Increasing pressure was also found to reduce the wall thickness and size of the pores. It induced channels within the structure of the elastin hydrogels that promoted fibroblast penetration and proliferation.(62)

CO_2 has been mainly used in hydrogels for the formation of pores within the scaffolds and for hydrogel foaming. Using CO_2 provides control over the microstructure and size of the pores and also helps in accelerating the crosslinking time of the hydrogels.

2.5 Incorporation of Growth Factors and Mammalian Cells

As discussed in the previous section, there are many methods utilizing supercritical fluid technology to prepare 3D scaffolds. While these scaffolds provide some degree of mechanical integrity and are biocompatible on implantation, they alone may not be sufficient to promote cell adhesion, proliferation and differentiation into the desired tissue. They often require the presence of cell signaling molecules and other bioactive compounds. Research has been carried out to

encapsulate drug delivery molecules, bioactive signals and cells, and genes to promote cellular infiltration and differentiation using CO_2.

Hile *et al.*(63) were among the first to incorporate growth factors into polymeric foams using supercritical CO_2. They made porous poly(D, L-lactide-co-glycolide) containing basic fibroblast growth factor (bFGF) to promote angiogenesis. A homogenous water-in-solvent emulsion was prepared with the protein in the aqueous phase and the polymer in the organic phase. Saturating the emulsion with supercritical CO_2 followed by depressurization led to the formation of porous scaffolds encapsulated with the protein. The release rate of active bFGF from these porous scaffolds was not as high as that from salt leached scaffolds and there was greater solvent residue remaining. In a similar manner, drug delivery molecules can be encapsulated within a porous scaffold and used for cell culture.(64)

Duarte *et al.*(65) utilized a supercritical fluid impregnation method to prepare a chitosan scaffold containing dexamethasone. Loading of the bioactive compound was found to be most successful at a pressure of 8.0 MPa and a temperature of 35 ˚C, and increasing the pressure and temperature resulted in lower encapsulation efficiency. The release profile of dexamethasone was found to be sustainable.(65)

Kanczler *et al.*(66) encapsulated vascular endothelial growth factor (VEGF) in PLA scaffolds by supercritical foaming, and seeded them with human bone marrow stromal cells. They found that the combination of temporally delivering VEGF from scaffolds seeded with hBMSCs resulted in enhanced bone regeneration of a mouse femur segmental defect.

Alternatively, microparticles and nanoparticles can also be used as carriers for bioactive compounds. Santo *et al.* (67) demonstrated the utility of this technique in impregnating $P_{DL}LA$ with chitosan/chondroitin sulfate nanoparticles. The scaffolds were fabricated by supercritical fluid foaming at 200 bar and 35 ˚C. Homogeneous distribution of the nanoparticles was observed throughout the 3D scaffold. It was also noted that there was swelling (water uptake) of the construct due to the entrapment of the nanoparticles. The resultant scaffold was found to have adequate mechanical integrity, porosity and pore interconnectivity for supporting cells. *In vitro* studies revealed that this system could be used as a promising candidate for dual protein delivery systems for potential applications in tissue engineering.

Supercritical fluid technology is also being used to explore DNA delivery in polymeric foams for potential applications in tissue engineering. Nie *et al.*(68) is one such group that made use of supercritical CO_2 for plasmid delivery. In their study, PLGA/chitosan foams were made by combining the techniques of spray drying with supercritical CO_2. PLGA microspheres encapsulated with plasmid DNA were prepared using spray drying. The microspheres were then combined with chitosan molecules to form foams using supercritical CO_2. CO_2 pressure of 120 bar was used for a period of 2 hr after which the pressure was reduced to ambient conditions at a rate of 0.05 MPa/s. Sustained DNA release was observed from these scaffolds. The integrity of the plasmids was also found to be well maintained. While increasing the content of chitosan caused a decrease in the release rate of DNA, it proved to be helpful in facilitating cell adhesion and viability.

Processing of mammalian cells during supercritical CO_2 foaming of scaffolds was first tried by Ginty *et al.*(69) They developed a single-step supercritical CO_2 technique to prepare

PLA scaffolds that contained a cell suspension. Various mammalian cell types such as a myoblastic C2C12 cell line, 3T3 fibroblasts, chondrocytes and hepatocytes were investigated for their viability. Upon depressurizing, a polymer sponge containing viable cells was obtained. The functionality of C2C12 cells was demonstrated by their osteogenic response to the bioactive compound bone morphogenetic protein-2. While this is a convenient one-step process, the time-dependent survival of cells poses a major challenge. To overcome this issue of cell viability, Ginty *et al.*(70) developed a high pressure CO_2 injection port to deliver mammalian cells into an already plasticized scaffold during the foaming process. The cells were shown to be viable and were able to undergo osteogenic differentiation. In addition, the cells were able to retain both metabolic and enzyme activity.

Singh *et al.*(71) later formed microsphere based scaffolds containing cells by using sub-critical CO_2 sintering. Poly(lactide-co-glycolide) microsphere scaffolds were sintered using a subcritical CO_2 pressure of ~15 bar at 25 ºC for 1 hour followed by depressurization at a rate of ~0.14-0.21 bar/sec. During subcritical CO_2 sintering, the equilibration of CO_2 in the polymer is restricted due to the short exposure time and low pressure conditions, which leads to a comparatively reduced plasticized state than that achieved during gas foaming. The microspheres retained their spherical shape during this process and the slight swelling of the microsphere surfaces and subsequent adhesion (and possibly reptation) led to sintering of the adjoining microspheres, thereby resulting in a porous matrix. They applied this technology to form porous scaffolds that facilitated the growth of chondrocytes for cartilage tissue engineering applications. Cell viability during subcritical CO_2 sintering was also evaluated in this study. Human umbilical cord mesenchymal stromal cells (hUCMSCs) at a density of $1x10^6$ cells were mechanically

mixed with microspheres and exposed to CO_2 at a pressure of 30 bar for 4 min followed by depressurization at a rate of ~3 psi/sec. Viability tests revealed that almost the entire cell population survived the sintering process.

Carbon dioxide technology can hence be used to encapsulate a variety of compounds such as bioactive signals, drugs, and plasmids for gene delivery. In addition, CO_2 may also be used to incorporate cells into scaffolds as they are fabricated, performed in a single step.

2.6 Limitations of CO_2 Technology

Three dimensional scaffolds in tissue engineering provide a matrix for cell support, proliferation and differentiation. The presence of pores and interconnectivity between them helps the cells to proliferate, helps in nutrient and oxygen supply and waste removal. Therefore, pore architecture plays a crucial role in cell survival and production of ECM. Large pores help in nutrient supply and waste removal, but results in low cell attachment and intracellular signaling, whereas small pores have the opposite effect.(72, 73) Lack of porosity and interconnectivity in the scaffolds hampers cell growth. CO_2 technology offers the advantage of preparing 3D scaffolds without the use of harmful organic solvents, which are deleterious for cells. However, lack of control on pore size and pore interconnectivity and lack of mechanical integrity are some of the issues with some CO_2 technologies, which can limit their use. In addition, the presence of a non-porous skin layer over CO_2-foamed scaffolds is also a drawback. In this section, recent attempts to overcome some of the limitations of CO_2 technology will be discussed.

Tai *et al.*(74) identified the trends in pore growth and porosity by analyzing the effect of various parameters like soaking time, soaking pressure, soaking temperature, depressurization

rate, molecular weight and chemical composition of the polymer. They prepared a porous structure of PLA and PLGA by a CO_2 foaming process. The scaffolds had a non-porous skin layer present, which was removed prior to cell seeding and drug release studies. The results demonstrated that pore size decreased with increasing glycolic acid content for PLGA scaffolds. However, increasing glycolic acid content also resulted in lower porosity, with a maximum of 78% porosity obtained from PLGA scaffolds. Constructs made of polymers with low molecular weight (i.e., PLGA 85:15 with 15 kDa and PLGA 75:25 with 13 kDa) were found to be very fragile. A higher pressure and a longer soaking time facilitated the production of smaller pores as more CO_2 molecules diffused through the polymer matrix, thus leading to a higher nucleation density. Larger pores were obtained by increasing the temperature, as this increased the rate of diffusion, which allowed pore growth. Rapid depressurization resulted in the formation of large pores while increasing the rate of depressurization allowed pore growth.

Reverchon *et al.*(75) prepared a foamed PLLA scaffold that had an elevated porosity of above 90% with pore interconnectivity. Regarding mechanical integrity, the compressive modulus (Young's modulus determined from tensile experiments) was 81 kPa. The scaffolds were prepared by a three step process where a polymeric gel loaded with a solid porogen (in this case fructose) was first formed. The next step involved drying of the gel with supercritical CO_2, followed by washing with water to eliminate the porogen. Pore size was controlled by the size of the porogen added during the process.

Addition of microparticulate silica has been attempted to improve the pore interconnectivity in scaffolds prepared by supercritical CO_2 foaming.(2) It was found that by increasing the amount of silica particles in the polymer, smaller pores could be obtained that had

greater interconnectivity. Porosity was not affected by the presence of silica during CO_2 foaming.

Baker *et al.*(76) prepared porous resorbable polymer constructs by means of supercritical CO_2 processing that had structural and mechanical properties similar to human bone. A porous PDLGA construct was soaked in supercritical CO_2 followed by rapid depressurization. The constructs were then freeze-fractured with liquid nitrogen in the vertical and perpendicular directions. A lower CO_2 processing temperature of 35 ˚C helped form larger pores with thicker pore walls, while processing at 100 ˚C formed relatively smaller pores with a very low extent of pore interconnectivity. Using different CO_2 processing pressures had a similar effect on the pore architecture. It was reported that all of the constructs had a dense "cortical" shell about 15-20 μm thick with an interconnected porous "core" with pore diameters in the range of 236-239 μm. Mechanical integrity and water uptake capacity was found to be dependent on the glycolic acid content of the polymer.

Despite improvements in the pore architecture, use of gas foaming techniques still results in the formation of a non-porous skin layer. The rapid diffusion of the dissolved fluid out of the sample edges results in the formation of this dense, non-porous skin layer, which can be decreased by increasing the pressure.(77) Though the presence of this layer is not desirable for tissue engineering applications, it can be easily removed manually.(39) Porosity and pore size can be controlled using different pressures and temperatures. Higher pressure and longer soaking times can result in the formation of smaller pores. A longer depressurization rate can also help in smaller pore formation. Addition of porogens and silica has been found to improve pore interconnectivity.

2.7 Summary

The formation of scaffolds with desirable properties for tissue engineering applications remains a challenge. The conventional CO_2 foaming process has been developed extensively to prepare porous scaffolds with a high degree of porosity and pore interconnectivity from both natural and synthetic polymers. Process parameters such as temperature, pressure, depressurization rate, soaking time, venting time, and chemical properties of the polymer are governing factors for controlling the macro and micro-architecture of the 3D construct.

Preparation of 3D constructs that are able to reproduce the highly complex spatial organization of cells and extracellular matrix as seen in complex tissues is the need of the day. Scaffolds that are characterized by spatial gradients of porosity and pore size, (36) thereby mimicking the natural tissue, offer an interesting dimension to the latest developments in the field.

In conclusion, supercritical fluid technology offers an attractive alternative over conventional 3D scaffold fabrication techniques for formation of porous polymeric foams and incorporation of bioactive molecules without the use of organic solvents or high temperatures. The plasticizing and solvent properties of CO_2 have enabled it to be used in different research areas. A few key findings include the use of $scCO_2$ as a swelling agent for polymers to help impregnate the scaffold with desirable additives such as drugs and bioactive compounds as well as using CO_2 as a compressed fluid to obtain different polymer morphologies at lower temperatures and pressures less than 100 bar. Another major finding is the use of CO_2 at much

lower pressures to sinter together microspheres in the presence of cells. A variety of processing conditions for fabrication of scaffolds using CO_2 have also been reviewed here. The goal of CO_2 technology moving forward will be to extend it to provide a more complex and dynamic environment for tissue growth and development.

Chapter 3 Use of Subcritical CO_2 Sintering to Make Scaffolds from Microspheres of Different Polymeric Materials

3.1 Abstract

The aim of this study was to evaluate three-dimensional shape-specific microsphere based scaffolds comprising of poly(lactide-co-glycolide) (PLGA) and polycaprolactone (PCL) for bone and cartilage tissue engineering. Porous scaffolds composed of ~200 μm microspheres of either PLGA or PCL were prepared using dense phase CO_2 sintering, which were seeded with rat bone marrow mesenchymal stromal cells (rBMSCs), and exposed to either osteogenic (PLGA, PCL) or chondrogenic (PLGA) conditions for 6 weeks. The PCL microsphere based scaffolds supported cell adhesion and proliferation of the seeded cells, as revealed by scanning electron microscopy. With the osteogenic conditions, the PLGA constructs produced an order of magnitude more calcium (13.5 times more calcium at week 6), while the PCL constructs had far superior mechanical and structural integrity (125 times stiffer than PLGA at week 6) along with double the cell content of the PLGA constructs. Chondrogenic differentiation was limited in PLGA constructs, perhaps as a result of a degradation rate that was too high. The current study represents the first long-term culture of CO_2-sintered microsphere-based scaffolds, and has established important thermodynamic differences in sintering between the selected formulations of PLGA and PCL, with the former requiring adjustment of pressure only, and the latter requiring the adjustment of both pressure and temperature.

3.2 Introduction

In recent years, microsphere-based scaffolds have found a significant number of applications in the field of tissue engineering.(78-82) Microspheres offer the advantages of control over release rate of the encapsulated drug, degradation kinetics of the polymer and ease of fabrication.(83) Scaffold properties can be tailored by altering the microsphere design. Further control over the macromechanical and degradability properties of the scaffold can be achieved by selecting a suitable polymeric raw material. Poly(lactic-co-glycolic acid) (PLGA) and polycaprolactone (PCL) are two polymers that have been extensively used for various applications such as in drug delivery, diagnostics and other applications of clinical and basic science research, including cardiovascular disease, cancer, vaccine and tissue engineering. (84) These polymers offer control over the degradation properties, which can be modified by altering one or more factors such as molecular weight, co-polymer ratio, tacticity, crystallinity, etc.(85, 86)

Techniques used to prepare microsphere-based scaffolds include solvent casting/ particulate leaching,(24) solvent/non-solvent treatment (using acetone and ethanol),(87) heat sintering (27, 28) and an anti-solvent sintering technique using ethanol.(88) Each of these methods has its own advantages, but they mostly make use of large amounts of organic solvents and/or exposure to elevated temperatures, which limit their use. CO_2 technology provides an attractive alternative to these traditional methods of scaffold fabrication. CO_2 has been widely used since it has a low critical temperature (T_c=31.1 ˚C and P_c=73.8 bar), which makes it suitable for processing thermo-sensitive compounds. It has the advantages of being inexpensive, non-

toxic and non-flammable. The recovery of final products and removal of CO_2 can be done easily with no residue left behind.(10)

Continuing upon the work of Singh *et al.* and utilizing the plasticizing properties of CO_2 to produce scaffolds using monodisperse microspheres,(89) the goal of the present study was to induce osteogenesis and chondrogenesis over a 6 week culture period using rat bone marrow mesenchymal stromal cells (rBMSCs). An additional purpose of this study was to examine the sintering of microspheres of either PLGA or PCL, with the former requiring adjustment of pressure only, and the latter requiring the adjustment of both pressure and temperature.

3.3 Materials and Methods

3.3.1 Scaffolding materials

Poly(D,L-lactic acid-co-glycolic acid) copolymer (PLGA) having a lactide:glycolide content of 50:50, molecular weight (MW) ~42,000-44,000 Da, and an intrinsic viscosity of 0.37 dL/g was purchased from Lakeshore Biomaterials (Birmingham, AL). Poly(ε-caprolactone) (PCL) having an intrinsic viscosity of 1-1.3 dL/g and MW of ~110,000-125,000 Da was purchased from LACTEL Absorbable Polymers (Birmingham, AL). Poly(vinyl alcohol) (PVA; 88% hydrolyzed, MW~25,000 Da) was purchased from Polysciences, Inc. (Warrington, PA). Dichloromethane (DCM; HPLC grade) was obtained from Fisher Scientific (Pittsburgh, PA).

3.3.2 Preparation of microspheres

Uniform PLGA and PCL microspheres were prepared by a method that was introduced by previous members in the group. (88, 90, 91) Briefly, using acoustic excitation produced by an ultrasonic transducer, regular jet instabilities were created in the polymer stream that produced uniform polymer droplets. An annular carrier non-solvent stream (0.5% w/v PVA) in double distilled water, ddH_2O) surrounding the droplets, was produced using a nozzle coaxial to the needle. The polymer/carrier streams flowed into a beaker containing the non-solvent. The polymer droplets were stirred for 3-4 hours to allow solvent evaporation, which were then filtered and rinsed with distilled water to remove residual PVA, and stored at -20 ºC. The particles were then lyophilized for 48 hrs and stored. A 10% polymer solution for PCL and 20% polymer solution for PLGA were used to prepare the microspheres.

3.3.3 Scaffold fabrication

Scaffolds were fabricated by exposure to sub-critical levels of CO_2 in a custom-designed stainless steel vessel having a pressure safety rating of 60 bar. Specific amounts of microspheres (80 mg of PLGA or 60 mg of PCL microspheres) were loaded into a Teflon mold and exposed to CO_2. Based on parameters selected following preliminary studies, PLGA microspheres were exposed to a CO_2 absolute pressure of 364 psi (~25 bar) at room temperature for a period of 1 hour followed by depressurization at the rate of 0.101 psi/s for 1 hour. Various combinations of temperature, pressure and exposure time were investigated for PCL scaffold fabrication (Appendix D). Following this, exposure to an absolute pressure of 690 psi (47.6 bar) at 45 ºC for a period of 4 hours followed by depressurization at a rate of ~0.2 psi/s for 1 hour was found to be optimum for PCL scaffold fabrication. The target was to obtain a comparable degree of

sintering between PLGA and PCL as evidenced by porosity, SEM imaging and integrity over 1 week in PBS at 37ºC. Scaffolds of the dimensions 7.5 ± 0.2 mm diameter and 2.5 ± 0.2 mm height were obtained by this method. Scaffolds were stored at room temperature until further use. The porosities of the cylindrical scaffolds were calculated as:

$$Porosity = (1-\rho_{app}/\rho) \times 100\% \quad (1.0)$$

Where ρ_{app} is the apparent density of the scaffold, given by $\rho_{app} = 4\,m/\pi d^2 h$, ρ is the density of the stock PLGA or PCL, m is mass of the cylindrical scaffolds, h is thickness and d is the diameter.

3.3.4 Scanning electron microscopy (SEM)

Scaffolds in culture were fixed in glutaraldehyde followed by dehydration in ethanol. Critical point drying of both PLGA and PCL scaffolds was done by dissolving in hexamethyldisilazane (HMDS) for 30 min followed by coating with a gold/palladium target. The imaging was performed using a Leo 1550 field emission scanning electron microscope at an accelerating voltage of 5 kV under a high vacuum.

3.3.5 Cell harvest

Rat bone marrow stem cells (rBMSCs) were obtained from the femurs of fifteen young male Sprague-Dawley rats (176-200 g, SASCO) following a University of Kansas approved IACUC protocol (175-08). Briefly, all rats were euthanized by exposure to CO_2 for 5 minutes followed by removal of the leg bones. The femur was then separated from the tibia and all excess muscle was removed. The marrow cavity was then flushed out of the femur using a

syringe filled with 1% Antibiotic-Antifungal/PBS solution. All cells obtained were plated for expansion in monolayer up to P1 and incubated at 37 ºC (NuAire, Autoflow, 5% CO_2, 90% humidity). The culture medium for rBMSCs was composed of Alpha MEM, 1% Penicillin-Streptomycin (both from Invitrogen Life Technologies, Carlsbad, CA), 10% fetal bovine serum qualified (FBS; Gemini, West Sacramento, CA) and was changed every 2-3 days. After the second passage (P2), the cell solution was re-suspended at the density of 1 million cells per mL of the freezing medium (Cell Culture Freezing Media DMSO, Fisher Scientific). The cell suspensions were transferred to cryotubes and stored at -80 ºC overnight in Mr. Frosty freezing containers (Nalgene, Rochester, NY). The cell suspensions were later transferred to a liquid nitrogen cryogenic storage tank at -196 ºC for future use.

3.3.6 Description of experimental groups

The study groups were divided into four categories. All scaffolds were seeded with rBMSCs. The first group consisted of a PLGA control that was cultured in plain BMSC media in the absence of growth factors. Two groups were cultured in osteogenic media (described below), either PLGA or PCL. Finally, the last group consisted of PLGA scaffolds cultured in chondrogenic media (described below) with the presence of TGF-β3 in the culture media.

3.3.7 Cell seeding

Frozen rBMSCs were thawed and plated at a density of 40,000 cells/cm^2. When the flasks were about 80-90% confluent, they were trypsinized and re-plated at the same density and expanded up to P4 in 300 cm^2 flasks. The cells were then re-suspended and seeded at a density of 10 million cells/mL of the scaffold. Scaffolds were sterilized by ethylene oxide prior to seeding.

After sterilization, the scaffolds were air dried in a fume hood for 1 day and placed in a 24-well plate. All scaffolds were evenly distributed among all groups. 55.2 μL (50% of the scaffold volume, which approximately corresponds to the pore volume (88)) of the cell suspension was placed directly on top of the scaffolds, allowing cells to penetrate into the scaffold via capillary action. The cells were then allowed to attach for 3 hours and the scaffolds were denoted as "week 0" at this point of time. 1.5 mL of the respective culture media was then added to all scaffolds and they were cultured statically. The culture medium for the PLGA control group consisted of alpha MEM, 1% penicillin-streptomycin (both from Invitrogen Life Technologies, Carlsbad, CA) and 10% fetal bovine serum qualified (FBS; Gemini, West Sacramento, CA). Both PLGA and PCL osteogenic groups were cultured in medium consisting of Dulbecco's modified Eagle medium (DMEM-LG; Invitrogen, Carlsbad, CA), 1% penicillin-streptomycin, 10% fetal bovine serum qualified, 50 μg/mL L-ascorbic acid (Sigma), 10 nM 1 α,25 dihydroxyvitamin D3 (Biomol International, Plymouth Meeting, PA), 10 mM β-glycerophosphate (disodium salt, pentahydrate; Calbiochem, San Diego, CA), 0.1 μM dexamethasone and 50 ng/mL BMP-2 (Peprotech, Inc., Rocky Hill, NJ). The PLGA chondrogenic group was cultured in medium composed of DMEM-high glucose (Invitrogen), 1X insulin-transferrin-selenium (ITS)-premix (BD Biosciences, San Jose, CA), 50 μg/mL L-ascorbic acid (Sigma), 1% penicillin-streptomycin, 40 μg/mL L-proline, 100 μM sodium pyruvate (Fisher Scientific, Pittsburgh, PA), 1% non-essential amino acids (NEAA) (Invitrogen) and 10 ng/mL transforming growth factor (TGF)-β3. TGF-β3 and BMP-2 are widely used for inducing chondrogenesis (92, 93) and osteogenesis,(94, 95) respectively, and hence were used in soluble form in the media. Media were replaced for all constructs every 48 hrs. After 3 weeks in culture, 15 mM HEPES buffer (Fisher Scientific) was added to all groups to control the pH.

3.3.8 Biochemical analyses

At weeks 0, 3 and 6, constructs (n=4) were analyzed for matrix production using biochemical assays. The constructs were digested by adding 1.2 mL of papain solution comprising of 125 μg/mL papain (from papaya latex, Sigma), 5 mM *N*-acetyl cysteine, 5 mM ethylenediaminetetraacetic acid (EDTA), and 100 mM potassium phosphate buffer in ddH_2O (20 mM monobasic potassium phosphate, 79 mM dibasic potassium phosphate in ddH_2O). The constructs were placed in microcentrifuge tubes containing papain solution and left overnight at 60 ºC. After digestion, the scaffolds were centrifuged at 10,000 rpm for 5 minutes to form a pellet of the polymer and other impurities and later stored at -20 ºC for biochemical analysis. The supernatant was later used to analyze DNA, and hydroxyproline (HYP) content, and for the chondrogenic and control groups, also glycosaminoglycan (GAG) content.

The DNA content was analyzed using a PicoGreen kit (Molecular Probes, Eugene, OR) according to the manufacturer's protocol. GAG content, which is an important component of connective tissues such as cartilage, was determined using a dimethylmethylene blue (DMMB) assay kit according to the manufacturer's instructions (Biocolor, Newtownabbey, Northern Ireland). Briefly, about 1 mL of DMMB was added to 100 μL of each sample and allowed to bind for 30 minutes. The pellet was then collected via centrifugation and resuspended and read at 656 nm. Hydroxyproline content, a major component of collagen, was determined using a modified HYP assay method.(96) Briefly, 400 μL of each sample was hydrolyzed with an equal volume of 4N NaOH at 121 ºC for 30 min. It was then neutralized with an equal volume of 4N HCl and titrated to a pH of 6.5-7. Approximately 500 μL of this solution was combined with an equal volume of chloramine-T solution buffer comprising of 50 g/L citric acid, 120 g/L sodium

acetate trihydrate, 34 g/L sodium hydroxide and 12.5 g/L acetic acid. The resultant solution was later combined with 500 µL of 1.17 mM p-dimethylaminobenzaldehyde in perchloric acid and read at 550 nm. A conversion factor of 11.5 can be used to convert the hydroxyproline mass to collagen content based on our previous studies.

To determine alkaline phosphatase (ALP) activity and calcium content for the osteogenic and control groups, constructs (n=4) were homogenized in 1 mL of 0.05% Triton X-100 (Sigma) and stored at -20 ºC. Elevated ALP activity is an indicator of active bone formation as ALP is a byproduct of osteoblast activity. To analyze the ALP activity, the plates were lysed twice using the freeze-thaw cycles. About 20 µL of the lysate was then combined with 100 µL 2-amino-2-methyl-1-propanol (AMP) buffer and incubated at 37 ºC for 75 min. The wells turned yellow, following which the reaction was stopped by the addition of 100 µL of 0.5M NaOH and subsequently read at 405 nm. The total ALP activity was expressed as a measure of liberated p-nitrophenol concentration/µg protein/min, as described elsewhere.(97) The protein content was determined by combining 20 µL of the lysate with 40 µL BioRad reagent and subsequent reading at 600 nm.

Calcium content was determined by using QuantiChrom^{TM} Calcium Assay Kit (DICA-500; QuantiChrom) according to the manufacturer's instructions.

3.3.9 Quantitative polymerase chain reaction

Reverse transcriptase-polymerase chain reaction (RT-PCR) was performed on scaffolds as a measure of gene expression. To perform RT-PCR, scaffolds (n=4) at weeks 0, 1, 2, 3 and 6 were homogenized in 1 mL of Trizol reagent (Invitrogen) and preserved at -80 ºC. RNA was

later isolated according to the manufacturer's instructions and converted to cDNA using a TaqMan High Capacity kit (Applied Biosystems, Foster City, CA) in a BioRad ThermoCycler. Assay IDs of TaqMan gene expression assays were Hs00164004_m1 for COL1A1, Hs00173720_m1 for IBSP, Hs00231692_m1 for RUNX2, Hs00202971_m1 for ACAN, Hs00165814_m1 for SOX9, Hs00156568_m1 for COL2A1 and Hs99999905_m1 for glyceraldehyde 3-phosphate dehydrogenase (GAPDH) and this reaction was carried out in an Applied Biosystems 7500 Fast Real-time PCR System. A $2^{-\Delta\Delta Ct}$ method was used to evaluate the relative level of each target gene.(98) For quantification purposes, the control PLGA group at week 0 was designated as the calibrator group, with GAPDH expression as an endogenous control.

3.3.10 Histological staining

Samples from week 3 and week 6 (n=3) for all groups except Osteogenic PCL were removed from the culture and placed in Optimal Cutting Temperature (OCT, Tissue-Tek) embedding medium and allowed to equilibrate overnight at 37 ºC. The samples were then preserved at -20 ºC for future use. 16 µm thick sections were cut perpendicular to the construct axis using a cryostat (Micron Hm-550 OMP, Vista, CA) and collected on SuperFrost Plus slides (Fisher Scientific). The slides were fixed in chilled acetone prior to staining.

Methyl methacrylate (MMA) embedding was carried out for the Osteogenic PCL constructs (n=3) from week 3 and 6, which was done because frozen sectioning of these constructs was not possible. The cryo-sectioning embedding medium was softer than the constructs. They were fixed in 10% neutral buffered formalin for 1 day followed by dehydration

in graded alcohol for 6 hours. The samples were then immersed in infiltrate solution in a glass vial and left for 1 day at room temperature on a shaker. The infiltrate solution comprised of 8.4 mL methyl methacrylate, 1.4 mL dibutylphthalate, 100 µL polyethylene glycol 400 (PEG 400) and 70 mg benzoyl peroxide (BPO) for each specimen. Following infiltration, the samples were placed in individual glass vials consisting of 10 mL of embedding solution and placed at 4 ºC for 3 days. The embedding solution (n=1) was made up of 8.4 mL methyl methacrylate, 1.4 mL of dibutylphthalate, 100 µL polyethylene glycol 400 (PEG 400), 40 mg benzoyl peroxide and 33 µL of N,N-dimethyl-ptoludine (DMT). Sectioning of the plastic embedded scaffolds was carried out using a microtome (Thermo Scientific Microm HM355S microtome). About 10 µm thick sections were obtained and placed on gelatin coated slides. They were covered with a precut piece of polyethylene film to make the sections flat and placed in a 42-45 ºC incubator for one day. Prior to staining, the polyethylene film was removed and all of the slides were deplasticized in 2-methoxyethylacetate followed by acetone and deionized water.

Safranin-O/Fast Green staining for GAGs, Alizarin Red for calcium depositions and von Kossa staining for calcium phosphate deposition and Hematoxylin and Eosin staining for cell nuclei and ECM was carried out on all samples. Finally, the slides were dehydrated in graded alcohol (95% and 100% ethanol, twice each) and cleared in xylene prior to mounting.

Immunohistochemistry (n=3) was also performed for types I and II of collagen in a BioGenex i6000 autostainer (BioGenex, San Ramon, CA). Slides were hydrated with PBS for 5 min. Endogenous peroxidase activity was inhibited using 1% hydrogen peroxide in methanol for 30 min. Each section was then blocked with a 3% horse serum solution for 30 min followed by

incubation with a primary antibody for 1 hour. Mouse monoclonal IgG anti-collagen I (1:1500 dilution; Accurate Chemical and Scientific, Westbury, NY) and mouse monoclonal IgG anti-collagen II (1:1000 dilution; Chondrex, Redmond, WA) were the primary antibodies used in this study. Following primary antibody incubation, the sections were incubated with a streptavidin-linked horse anti-mouse IgG secondary antibody (Vector Laboratories, Burlingame, CA) for 30 min. The sections were then incubated with an avidin-biotinylated enzyme complex (ABC complex; Vector Laboratories) for 30 min, and later with VIP substrate (purple color) (Vector Laboratories) for 10 min. Negative controls with the primary antibody omitted were also run.

3.3.11 Mechanical testing

Mechanical characterization of the constructs (n=5) was carried out using a uniaxial testing apparatus (Instron Model 5848, Canton, MA, 50 N load cell) under unconfined compression using a custom-built bath-platen apparatus (99). Cylindrical scaffolds prepared by CO_2 sintering were tested under simulated physiological conditions (i.e., phosphate buffered saline (PBS) comprised of 0.138 M sodium chloride, 0.0027 M potassium chloride at 37 ºC). At week 0, cell-seeded scaffolds of PCL and one group of PLGA were tested (7.8 ± 0.2 mm diameter, 1.7 ± 0.7 mm height for PCL constructs; 8.3 ± 0.3 mm diameter, 1.8 ± 0.5 mm height for PLGA constructs). It was assumed that there would be no detectable differences in the mechanical properties of the three PLGA groups at week 0 given that those scaffolds were all identical. At week 6, all four groups were tested. The dimensions of the constructs at week 6 were 13.7 ± 1.4 mm diameter, 1.1 ± 0.5 mm height for the Control PLGA constructs. The Chondrogenic PLGA group were 13.6 ± 1.2 mm in diameter and 2.5 ± 0.8 mm in height. The osteogenic groups had a diameter of 11.8 ± 1.7 mm and a height of 1.9 ± 0.6 mm height for the PLGA group and a

diameter of 7.5 ± 0.2 mm and a height of 1.9 ± 0.4 mm for the PCL group. Compressive moduli of elasticity were obtained from the linear regions of the stress-strain curves. A continuous deformation rate of 5 mm/min was used during the compression testing. The stress was defined as the ratio of the load to the initial cross-sectional area, and the strain was defined as the ratio of the change in length to the original length.

3.3.12 Statistical analyses

Statistical analyses were performed using a single factor analysis of variance with a Tukey's post hoc test (ANOVA) in Origin 6.0 software. All quantitative results (numerical values and representative diagrams) were expressed as the average ± standard deviation.

3.4 Results

3.4.1 Microspheres and scaffold fabrication

PLGA and PCL microspheres having uniform diameter were prepared using Precision Particle Fabrication method.(90) The microspheres displayed high monodispersity and had a nominal diameter of ~200 μm.

Cylindrical scaffolds containing two types of polymers, PLGA and PCL, were produced using subcritical CO_2 as previously described. Morphological assessment of the scaffolds using scanning electron microscopy (SEM) revealed that there were slight distortions on the surfaces of the microspheres, but the spherical shape was largely retained as seen in Figure 3. SEM

images of the Chondrogenic PLGA group were not available as they were unable to withstand SEM processing. The microsphere matrices were also found to be porous. Scaffolds with a final diameter of 7.5 ± 0.2 mm and a height of 2.5 ± 0.2 mm were formed resulting in a scaffold volume of 110.4 μL. The porosity was calculated according to equation (1) and was found to be 44.6 ± 4.1% for PCL scaffolds and 43.2 ± 0.2% for PLGA scaffolds (no statistically significant difference). SEM imaging after 6 weeks showed that PCL microspheres retained their spherical shape while PLGA microspheres completely degraded (Figure 3).

3.4.2 DNA content

The overall DNA content for all constructs decreased over the period of 6 weeks ($p < 0.05$) as seen in Figure 4. There was a statistically significant decrease in DNA content for each group at weeks 3 and 6 compared to their week 0 values. The three PLGA groups decreased by 70% at week 6 ($p < 0.005$) compared to their week 0 values while the Osteogenic PCL group decreased by 38% at the end of week 6 ($p \leq 0.01$). However, the DNA content in the Osteogenic PCL group was found to be significantly higher than the Control PLGA group at weeks 3 and 6. There was 2.0 times higher DNA contents in the Osteogenic PCL group compared to the Control PLGA group at weeks 3 ($p < 0.005$) and 6 ($p \leq 0.01$), respectively. The average DNA contents in the remaining three groups were found to be similar to each other at week 6.

3.4.3 Glycosaminoglycan content

GAG analysis was carried out on only two groups: Control PLGA and Chondrogenic PLGA. Statistically significant differences in the GAG content were not observed in either group over time (Figure 5).

3.4.4 Hydroxyproline content

The hydroxyproline (HYP) data for all groups is shown in Figure 6. Statistically significant differences in the absolute HYP were not observed for any group during the 6 weeks.

All of the three PLGA groups showed a significant increase in HYP/DNA content at weeks 3 and 6 compared to the week 0 Control PLGA group ($p < 0.01$). No significant changes were observed in the Osteogenic PCL group throughout the 6 weeks. However, its value was observed to be 1.9 times lower than the Control PLGA group at week 3 ($p < 0.01$) and week 6 ($p < 0.05$). By 3 weeks, the Control PLGA and the Chondrogenic PLGA constructs made 3.0 times ($p < 0.005$) and 4.2 times ($p < 0.001$), respectively, more HYP/DNA than their previous time point. The Osteogenic PLGA constructs showed no significant increase in HYP/DNA content at week 3 compared to its week 0 value. However, at 6 weeks, the Osteogenic PLGA group had 2.3 times higher HYP/DNA content ($p \leq 0.001$) than the week 0 Control PLGA group. Significant differences between the two osteogenic groups were not observed.

3.4.5 Calcium content

Calcium content for all constructs showed no statistically significant changes until week 2 (Figure 7). At week 2, the Osteogenic PLGA group increased 22 times over its week 0 value ($p \leq 0.02$), the Control PLGA group increased by a factor of 5.1 ($p < 0.001$) while Osteogenic PCL group did not change significantly. The Osteogenic PLGA group had 6.2 times more calcium than the control group at week 6 ($p < 0.001$) and 10.0 times more than the Osteogenic PCL group ($p < 0.001$) at week 6.

Normalized data showed a similar trend with increases in calcium content from week 2 onward. The Osteogenic PLGA and Control PLGA groups had significantly higher calcium contents at week 2 (35.9 times higher, $p \leq 0.02$ for Osteogenic PLGA; 12.6 times higher, $p < 0.001$ for Control PLGA) and week 3 (44.6 times higher, $p < 0.001$ for Osteogenic PLGA; 21.3 times higher, $p \leq 0.05$ for Control PLGA) compared to the their week 0 value. The Osteogenic PCL group did not show any significant increase in calcium content over its week 0 value ($p > 0.05$). Calcium content in the Osteogenic PLGA group was found to be significantly higher when compared to the PCL group at weeks 2 (10.2 times higher, $p \leq 0.03$), 3 (12 times higher, $p < 0.001$) and 6 (13.5 times higher, $p < 0.001$).

3.4.6 Alkaline phosphatase activity

The Osteogenic PCL and PLGA groups had significantly lower ALP activity than the Control PLGA group at weeks 0 and 1 (Figure 8). The Control PLGA group showed a 64% decrease in its ALP activity ($p \leq 0.002$) at the end of 6 weeks when compared to its week 0 value, and the Osteogenic PLGA group also experienced a decrease in ALP activity from week 0 to week 6, being 82.6% lower ($p < 0.005$). However, the ALP activity of the Osteogenic PCL constructs increased by 2.0 times at the end of 6 weeks relative to its week 0 value ($p \leq 0.03$). The ALP activity of the Osteogenic PCL group was found to be 2.3 times higher than the Osteogenic PLGA group at week 3 ($p < 0.001$) and 5.8 times higher at week 6 ($p < 0.001$).

3.4.7 Gene expression

All treatment groups showed a slight increase in COL1A1 expression over the period of 6 weeks (Figure 9). There was observed to be a 21.3 fold increase in COL1A1 expression for the

Osteogenic PCL group at week 3 over its week 1 value ($p < 0.005$). Significant changes in expression over the previous time points were not observed for the Osteogenic PLGA group. However, its expression was significantly lower than the Control PLGA group at week 1 (6.1 times lower, $p \leq 0.02$) and week 3 (5.04 times lower, $p \leq 0.02$). A significant difference was observed between the two osteogenic groups at weeks 3 and 6 ($p < 0.05$). COL1A1 expression was found to be 7.0 times higher in the Osteogenic PCL group than in the Osteogenic PLGA group at week 6 ($p < 0.05$).

Statistically significant changes in COL2A2 expression were observed in all groups over the period of 6 weeks (Figure 10). The chondrogenic PLGA group exhibited an 11 fold increase in expression at week 1 over its week 0 value ($p < 0.01$). Statistically significant changes in expression were also seen between the two osteogenic groups at week 1. The Osteogenic PCL group had 123 times higher expression ($p \leq 0.001$) than the Osteogenic PLGA at week 1.

Runx2 expression increased 10.1 times at week 3 over its week 1 value for the Osteogenic PCL group, and decreased later at week 6 ($p < 0.001$) while the Osteogenic PLGA group showed a 3.7 times increase at week 6 over its week 1 value ($p < 0.001$). Runx2 expression of the Osteogenic PLGA group at week 3 could not be detected. Significant differences in Runx2 expression were not observed between the two osteogenic groups (Figure 11).

No significant changes were observed in aggrecan expression throughout the culture period (Figure 12). The highest expression in all four groups was observed at week 3 with values

decreasing later at week 6 (not statistically significant). Significant differences in expression between the two osteogenic groups were not observed.

Relative expressions of Sox-9 and BSP gene were not reported due to their low gene expression values.

3.4.8 Histological staining

Staining for cell nuclei with Hematoxylin & Eosin (H&E), Safranin-O/Fast Green for GAG content, Alizarin Red for calcium deposition and von Kossa for calcium phosphate was carried out on all groups. At 3 weeks (Figure 13), all constructs demonstrated a negligible degree of Saf-O staining, with the Osteogenic PCL group having some staining detected near the periphery of the microspheres. Cell nuclei, visualized by H&E staining, were present mainly toward the periphery of the scaffolds. Visualization of cells was particularly difficult with the Chondrogenic PLGA constructs. Alizarin Red staining seemed to be present almost throughout the construct, with the highest concentration in the edges of the scaffolds for all groups, except for the Chondrogenic PLGA group. The Control PLGA and Osteogenic PLGA groups showed more intense staining for calcium, both staining more intensely than the Osteogenic PCL group. von Kossa staining was used to identify the presence of calcium phosphate deposits in the constructs. At week 3, the Osteogenic PLGA group showed the presence of von Kossa staining distributed throughout the construct. The control PLGA construct also exhibited some von Kossa staining to a lesser extent, and traces of von Kossa staining were seen in the Chondrogenic PLGA group. It was difficult to discern any von Kossa staining in the Osteogenic PCL group at week 3.

By 6 weeks (Figure 14), the density of cell nuclei decreased in all groups except for the Osteogenic PLGA group, which had a larger number of cells near the outer boundary of the construct. In addition, Saf-O staining was only observed in the Osteogenic PCL group while Alizarin Red staining was most prominent in the Control PLGA group, particularly around the periphery. The Osteogenic PLGA group also showed noticeable staining for Alizarin Red, however to a somewhat lesser extent, with slightly more intense staining around the periphery as well. Alizarin Red staining was observed in trace amounts in the Chondrogenic PLGA and the Osteogenic PCL groups. Non-uniform clusters of von Kossa staining were observed in all groups with the Control PLGA group being most intensely stained, followed by the Osteogenic PLGA group.

Immunohistochemistry was also carried out on all treatment groups at weeks 3 and 6 (Figure 15). By 3 weeks, positive immunostaining was observed for type I collagen with relatively more staining in the Osteogenic PCL group, followed by the Control and Osteogenic PLGA groups, with minimal staining for the Chondrogenic PLGA group. The presence of type II collagen was seen mostly in the Control PLGA group and even to some extent in the Osteogenic PCL group. By 6 weeks, both type I and type II collagen were seen in all groups with the most intense staining in the control group followed by the Osteogenic groups and the least staining in the Chondrogenic PLGA group.

3.4.9 Mechanical testing

The representative stress-strain curves from unconfined compression testing for all groups at week 0 and week 6 have been shown in Appendix C. All the groups except week 6 Osteogenic

PCL group showed an initial linear region followed by a nonlinear collapse region. The Osteogenic PCL group at week 6 behaved differently. The compressive moduli were determined from the stress-strain plots using the initial linear regions which were arbitrarily chosen, before the onset of the nonlinear region which generally extended up to 40% strain for all the PLGA groups, while the week 0 Control PCL and PLGA groups were linear up to 20% strain. For the week 6 PCL group, the modulus of elasticity was calculated from the initial linear region that extended up to only 10% strain. Same strain range starting from 0 to 40% for all PLGA groups at week 6 and from 0 to 20% for week 0 groups were used ($n = 5$). The modulus of elasticity was determined to be 4.25 times higher for the PLGA constructs at week 0 (193.9 ± 47.4 kPa) than the PCL constructs (45.6 ± 26.3 kPa) at the same time point ($p < 0.001$). However, after 6 weeks the PCL constructs (79.8 ± 6.7 kPa) were at least 125 times stiffer than the PLGA groups ($p < 0.001$). The moduli of the PLGA constructs (0.3 ± 0.1 kPa) dropped drastically after 6 weeks in culture. They decreased by 99.6% of their week 0 values at the end of week 6 ($p < 0.001$). On the other hand, the elastic modulus for the PCL constructs actually increased by 75% from week 0 to week 6 (not statistically significant).

3.5 Discussion

The overall objective of this study was to investigate the use of a novel microsphere based scaffold formed by subcritical CO_2 sintering for osteogenic and chondrogenic tissue engineering. Two commonly used polymeric scaffold materials PLGA and PCL were used in this study. Subcritical CO_2 sintering (~25 bar for PLGA at 25ºC and ~47 bar for PCL at 45ºC) was used to

prepare scaffolds due to the high solubility of CO_2 in polymers and its ability to plasticize polymers by lowering the glass transition temperature or melting point.(16) From the SEM images at week 0 and the porosity data, comparable degrees of sintering were observed in both PCL and PLGA constructs. Since the molecular structure and morphology of the polymers greatly influence CO_2 solubility and diffusivity, PLGA having more accessible free volume (due to lesser steric hindrance) may have a greater solubility in CO_2 than PCL.(8) Perhaps due in part to this steric hindrance with PCL, a shorter equilibration time with CO_2 was needed for PLGA (1 hour), while PCL needed a relatively longer time (4 hours) at a higher pressure and slightly elevated temperature of 45ºC. Due to the relatively short exposure time, plasticization of the entire polymer was avoided and the microspheres were only fused with each other, thereby retaining their spherical shape. A moderate depressurization rate was found to be desirable (0.101 psi s^{-1} for PLGA scaffolds and ~0.2 psi s^{-1} for PCL scaffolds) for the production of sintered matrices. Instantaneous depressurization was avoided because that would result in foaming of the prepared scaffolds. During depressurization, thermodynamic instability occurs within the polymer, resulting in nucleation of gas cells. These gas cells give rise to nanopores within the scaffold. Faster depressurization rates could be applied in the future to increase porosity as well as porogens like NaCl can be added to increase the porosity.(34)

At week 6, the presence of cells and ECM was observed in PCL constructs. The slow degradation rate of PCL enabled the microspheres to retain their shape throughout the 6 weeks in culture and no acidic byproducts were released. On the other hand, PLGA has a faster degradation rate. Although the swelling rates, water uptake and degradation rates were not calculated here, it was observed that swelling and change in size occurred as early as ten days in

culture for the PLGA constructs. Changes in pH were also noticeable at this stage for the PLGA constructs, evidenced by medium color change. Hence, to prevent further damage to cells, HEPES buffer was added to the culture media around week 3 to maintain the pH around 7. In future studies, steps may be taken to maintain the culture medium near a pH of 7 at all times, either by buffering of the medium or by encapsulation of buffers such as sodium bicarbonate or calcium carbonate.(100)

During the culture period, a loss of cells was observed. It has been observed that the DNA content decreased in PGA meshes due to its rapid degradation rate.(101) It was noted that the degradation rate was not equal to the rate of extracellular matrix synthesis, resulting in a contraction of scaffolds. Since the cell number did not further decrease from week 3 onward, it indicates that a more stable construct may have been achieved. The cell loss might be responsible for the GAG loss in the Control PLGA constructs. However, the Chondrogenic PLGA constructs showed an increased GAG production after week 3. Net HYP content did not show any significant increases over the period of 6 weeks. However, the normalized data showed an interesting trend with increase in HYP from week 3 onward for all groups. At week 6, the Chondrogenic PLGA group had the highest HYP mass. In addition, the two osteogenic groups were not significantly different from one another with respect to the HYP content, but their level was less than the control. Increased calcium content was observed for the Osteogenic PLGA group after week 3, indicating an onset of mineralization in those constructs. In contrast, the Osteogenic PCL group did not show a significant increase in calcium content. It is known that during osteogenic differentiation of MSCs, ALP activity decreases at later times. (102) This early indication of osteogenic differentiation in the PLGA group may be the reason for the low

ALP activity. However, further investigations need to be carried out to figure out the reasons for the varying trend for the other groups.

There was a drastic drop in the mechanical integrity of the scaffolds at the end of the culture period for PLGA scaffolds (99% decrease). This was most likely a consequence of microsphere degradation, leading to disappearance of the sintering-sites. The slow degradation rate of PCL enabled those constructs to retain their microsphere shape and mechanical integrity throughout the culture period, which could have important implications *in vivo*.

Certain strategies may be implemented in future studies to improve the performance of constructs. First, selection of an adequate PLGA polymer having higher lactic acid content, higher molecular weight and T_g can be utilized in microsphere preparation to decrease the degradation rate of the polymer. Second, a bimodal distribution of microspheres can be used during scaffold fabrication (89) to improve the mechanical properties of the scaffold although this would result in lower porosity. Addition of nanocomposite materials such as calcium carbonate, hydroxyapatite, or tricalcium phosphate within the microspheres can also help in maintaining the pH changes that occur during PLGA degradation, as well as providing "raw materials" to the cells and regenerating tissues *in vivo*. Third, faster depressurization rates can be explored and porogens can be added during CO_2 sintering to improve porosity. Finally, cell attachment and viability can be improved by functionalizing the polymer with haptotactic cues such as Arg-Gly-Asp (RGD) or Tyr-Ile-Gly-Ser-Arg, (YIGSR) (103) or by encapsulating natural "raw materials" such as those noted earlier.

3.6 Conclusions

The feasibility of using a novel microsphere based scaffold sintered using subcritical CO_2 for osteogenic and chondrogenic tissue engineering has been demonstrated in this thesis. This work builds on the previous efforts of a student in our group with CO_2-sintered microsphere-based scaffolds (89), where cell viability was demonstrated, by completing a full 6-week *in vitro* study with both osteogenesis and chondrogenesis, as well as establishing sintering parameters for PCL.

In this investigation, temperature, pressure and exposure time were necessary to control for CO_2 sintering of PCL (higher temperature and pressure conditions with longer exposure time), as opposed to PLGA, which was sintered at ambient temperature and pressure conditions (for 1 hour exposure). The PLGA degradation rate for CO_2 sintered microspheres in this first study appeared to be too high, at the expense of chondrogenesis, which may be addressed in the future with encapsulated buffers and/or a slower degrading PLGA.

With osteogenesis, there were marked differences between the PLGA and PCL constructs. Specifically, the PLGA group produced an order of magnitude more calcium, while PCL retained its shape, size and mechanical integrity and had twice as many cells per construct at 6 weeks. Although the PCL group generally had a higher ALP activity, and even a higher level of Runx2 gene expression at 3 weeks, by 6 weeks the PLGA constructs had a higher Runx2 expression while the PCL group instead had a higher aggrecan expression.

The overall conclusion here is that PLGA may be the material of choice in a CO_2 sintering application, based on the drastically superior calcium content observed in osteogenesis and the

more straightforward sintering conditions (Controlling the pressure and exposure time at ambient temperature), but that both chondrogenesis and osteogenesis may benefit from a slower degradation rate and the encapsulation of growth factors, calcium-based nanoparticles, and/or buffers in the microspheres.

Acknowledgments

The present work was supported by NIH Grant R21 EB007313. We are grateful to Alan Walker for helping with the design and construction of the stainless-steel CO_2 chamber.

Chapter 4 Conclusion

Previous studies related to this work have successfully tested cell viability during the CO_2 sintering process and produced cell loaded patches and scaffolds. Potential of these scaffolds for cartilage tissue engineering was also shown. The studies in this thesis made the first attempt in using bone marrow mesenchymal stromal cells from rats for engineering bone and cartilage tissue using subcritical CO_2 sintered microsphere-based scaffolds.

Osteogenic and chondrogenic differentiation of rBMSCs was induced *in vitro* by the addition of BMP-2 and TGF-β3 respectively in the culture media. Biochemical analysis, gene expression and histology staining revealed tissue growth in the constructs. In this investigation, both temperature and pressure (along with time) were necessary to adjust for CO_2 sintering of PCL, as opposed to PLGA, which was sintered at ambient temperature. The PLGA degradation rate for CO_2 sintered microspheres in this study appeared to be too high, at the expense of chondrogenesis, which may be addressed in the future with encapsulated buffers and/or a slower degrading PLGA. With osteogenesis, there were marked differences between the PLGA and PCL constructs. The onset of mineralization could be seen in the Osteogenic PLGA group due to its high calcium value while the Osteogenic PCL group showed an increase in mechanical integrity of the constructs after 6 weeks in culture. PCL also retained its shape, size and mechanical integrity and had twice as many cells per construct at 6 weeks. Although the PCL group generally had a higher ALP activity, and even a higher level of Runx2 gene expression at 3

weeks, by 6 weeks the PLGA constructs had a higher Runx2 expression while the PCL group instead had a higher aggrecan expression.

The overall conclusion here is thus that PLGA may be the material of choice in a CO_2 sintering application, given the drastically superior calcium content in osteogenesis and the more straightforward sintering conditions (Controlling the pressure and exposure time at ambient temperature), but that both chondrogenesis and osteogenesis may benefit from a slower degrading polymer in the future.

Future work can include loading of growth factors within the microspheres thereby providing a spatiotemporal control over the release rates. The present study used growth factors in the soluble form in the medium. Encapsulating them within the microspheres would provide control over its release rate.

Improvements to the custom-made stainless steel CO_2 chamber can be made to make scaffolds more efficiently. The present equipment does not have an in-built temperature and pressure gauge hence, the parameters could not be accurately monitored. The experimental set-up could be modified to provide better temperature control during the sintering of PCL. A pressure regulator can also be added to accurately maintain the pressure inside the vessel at a constant value with fewer leaks. A viewing window can be added to the chamber to be able to monitor the sintering process visually.

Moderate depressurization rates of 0.1psi/sec for PCL and 0.2 psi/sec for PLGA were used in this study. Porosities of 42% were observed in both polymeric scaffolds. Using faster rates of

depressurization and different sizes of microspheres can also be investigated to improve porosity. Porogens like NaCl particles can also be mixed along with the polymer during the CO_2 sintering process to improve the porosity, which has been investigated to some extent by a former post-doctoral fellow, Ju in our group. Slightly higher porosities of 52.8±6.8% (50:50 PLGA with 25 wt% NaCl, CO_2 sintering at 25 bar for 1 hr) than that achieved in this study can be obtained with this improvement. Also, pore interconnectivity within the scaffolds can be investigated and improved as it may help with better cell attachment and proliferation. This was not addressed in the present study.

PLGA copolymers having a decreased degradation rate (higher lactic acid content, high molecular weight) can be used. The PLGA copolymer used in this study started degrading after 10 days in culture and resulted in a loss of cells due to the release of acidic byproducts. Inclusion of nano materials like calcium phosphate, hydroxyapatite or bioglass can be done to improve the mechanical properties of the polymeric scaffold. These nanomaterials will also be useful in controlling the fluctuations in the pH of the culture media during the degradation process.

More efficient cell seeding methods can be explored. Constructs can be functionalized with Arg-Gly-Asp (RGD) sequence to improve cell attachment. The cell seeding method used in the present study had a low seeding efficiency, with cell number decreasing after week 1. Only one cell source rBMSCs were used in the present study. In future, different cell sources like umbilical cord mesenchymal stromal cells (hUCMSCs) can be also investigated for their potential in bone and cartilage tissue engineering applications.

The results presented in this thesis lay a foundation to explore numerous applications using subcritical carbon dioxide sintering for tissue engineering applications.

REFERENCES:

1. Ahmed TA, Hincke MT. Strategies for articular cartilage lesion repair and functional restoration. Tissue Eng Part B Rev.16:305-29. 2010.

2. Collins NJ, Bridson RH, Leeke GA, Grover LM. Particle seeding enhances interconnectivity in polymeric scaffolds foamed using supercritical CO2. Acta Biomaterialia.6:1055-60. 2010.

3. Duarte A.R.C. RC, Vega-Gonzalez A., Duarte C.M., Subra-Paternault P.,. Preparation of acetazolamide composite microparticles by supercritical anti-solvent techniques. Int J Pharm.332:132-9. 2007.

4. Duarte ARC, Mano JF, Reis RL. Perspectives on: Supercritical Fluid Technology for 3D Tissue Engineering Scaffold Applications. Journal of Bioactive and Compatible Polymers.24:385-400. 2009.

5. Colton JS, Suh NP. Nucleation of microcellular foam: Theory and practice. Polymer Engineering & Science.27:500-3. 1987.

6. De Ponti R, Torricelli, C., Martini, A. and Lardini, E. Use of Supercritical Fluids to obtain Porous Sponges of Biodegradable Polymers. 1991.

7. Mooney DJ, Baldwin DF, Suh NP, Vacanti JP, Langer R. Novel approach to fabricate porous sponges of poly(D,L-lactic-co-glycolic acid) without the use of organic solvents. Biomaterials.17:1417-22. 1996.

8. Davies OR, Lewis AL, Whitaker MJ, Tai H, Shakesheff KM, Howdle SM. Applications of supercritical CO2 in the fabrication of polymer systems for drug delivery and tissue engineering. Advanced Drug Delivery Reviews.60:373-87. 2008.

9. Pasquali I, Bettini R, Giordano F. Solid-state chemistry and particle engineering with supercritical fluids in pharmaceutics. Eur J Pharm Sci.27:299-310. 2006.

10. Duarte A.R.C MJF, Reis R.L. Supercritical fluids in biomedical and tissue engineering applications: a review. International Materials Reviews.54:214-22. 2009.

11. Tomasko DL, Li H, Liu D, Han X, Wingert MJ, Lee LJ, et al. A Review of CO2 Applications in the Processing of Polymers. Industrial & Engineering Chemistry Research.42:6431-56. 2003.

12. Nalawade SP, Picchioni F, Janssen LPBM. Supercritical carbon dioxide as a green solvent for processing polymer melts: Processing aspects and applications. Progress in Polymer Science.31:19-43. 2006.

13. Royer JR, DeSimone JM, Khan SA. High-pressure rheology and viscoelastic scaling predictions of polymer melts containing liquid and supercritical carbon dioxide. Journal of Polymer Science Part B: Polymer Physics.39:3055-66. 2001.

14. Royer JR, Gay YJ, Adam M, DeSimone JM, Khan SA. Polymer melt rheology with high-pressure CO2 using a novel magnetically levitated sphere rheometer. Polymer.43:2375-83. 2002.

15. Royer JR, Gay YJ, Desimone JM, Khan SA. High-pressure rheology of polystyrene melts plasticized with CO2: Experimental measurement and predictive scaling relationships. Journal of Polymer Science Part B: Polymer Physics.38:3168-80. 2000.

16. Areerat S, Funami E, Hayata Y, Nakagawa D, Ohshima M. Measurement and prediction of diffusion coefficients of supercritical CO2 in molten polymers. Polymer Engineering & Science.44:1915-24. 2004.

17. Nalawade SP, Picchioni F, Marsman JH, Janssen LPBM. The FT-IR studies of the interactions of CO2 and polymers having different chain groups. The Journal of Supercritical Fluids.36:236-44. 2006.

18. Shah VM, Hardy BJ, Stern SA. Solubility of carbon dioxide, methane, and propane in silicone polymers. Effect of polymer backbone chains. Journal of Polymer Science Part B: Polymer Physics.31:313-7. 1993.

19. Oliveira NS, Dorgan J, Coutinho JAP, Ferreira A, Daridon JL, Marrucho IM. Gas solubility of carbon dioxide in poly(lactic acid) at high pressures: Thermal treatment effect. Journal of Polymer Science Part B: Polymer Physics.45:616-25. 2007.

20. Kim SS, Utsunomiya H, Koski JA, Wu BM, Cima MJ, Sohn J, et al. Survival and function of hepatocytes on a novel three-dimensional synthetic biodegradable polymer scaffold with an intrinsic network of channels. Ann Surg.228:8-13. 1998.

21. Tsang VL, Bhatia SN. Three-dimensional tissue fabrication. Adv Drug Deliv Rev.56:1635-47. 2004.

22. Malda J, Woodfield TB, van der Vloodt F, Wilson C, Martens DE, Tramper J, et al. The effect of PEGT/PBT scaffold architecture on the composition of tissue engineered cartilage. Biomaterials.26:63-72. 2005.

23. Moroni L, de Wijn JR, van Blitterswijk CA. Integrating novel technologies to fabricate smart scaffolds. J Biomater Sci Polym Ed.19:543-72. 2008.

24. Deville S, Saiz E, Tomsia AP. Freeze casting of hydroxyapatite scaffolds for bone tissue engineering. Biomaterials.27:5480-9. 2006.

25. Ghosh S, Viana JC, Reis RL, Mano JF. The double porogen approach as a new technique for the fabrication of interconnected poly(L-lactic acid) and starch based biodegradable scaffolds. J Mater Sci Mater Med.18:185-93. 2007.

26. Sultana N, Wang M. Fabrication of HA/PHBV composite scaffolds through the emulsion freezing/freeze-drying process and characterisation of the scaffolds. J Mater Sci Mater Med.19:2555-61. 2008.

27. Borden M, Attawia M, Khan Y, El-Amin SF, Laurencin CT. Tissue-engineered bone formation in vivo using a novel sintered polymeric microsphere matrix. J Bone Joint Surg Br.86:1200-8. 2004.

28. Yao J, Radin S, P SL, Ducheyne P. The effect of bioactive glass content on synthesis and bioactivity of composite poly (lactic-co-glycolic acid)/bioactive glass substrate for tissue engineering. Biomaterials.26:1935-43. 2005.

29. Gomes ME, Ribeiro AS, Malafaya PB, Reis RL, Cunha AM. A new approach based on injection moulding to produce biodegradable starch-based polymeric scaffolds: morphology, mechanical and degradation behaviour. Biomaterials.22:883-9. 2001.

30. Wu C, Luo Y, Cuniberti G, Xiao Y, Gelinsky M. Three-dimensional printing of hierarchical and tough mesoporous bioactive glass scaffolds with a controllable pore

architecture, excellent mechanical strength and mineralization ability. Acta Biomaterialia.7:2644-50. 2011.

31. Vivanco J, Slane J, Nay R, Simpson A, Ploeg H-L. The effect of sintering temperature on the microstructure and mechanical properties of a bioceramic bone scaffold. Journal of the Mechanical Behavior of Biomedical Materials.

32. Liang D, Hsiao BS, Chu B. Functional electrospun nanofibrous scaffolds for biomedical applications. Adv Drug Deliv Rev.59:1392-412. 2007.

33. De Ponti R, Torricelli, C., Martini, A. and Lardini, E. . Patent: Use of Supercritical Fluids to obtain Porous Sponges of Biodegradable Polymers. 1991.

34. Harris LD, Kim BS, Mooney DJ. Open pore biodegradable matrices formed with gas foaming. J Biomed Mater Res.42:396-402. 1998.

35. Barry JJ, Gidda HS, Scotchford CA, Howdle SM. Porous methacrylate scaffolds: supercritical fluid fabrication and in vitro chondrocyte responses. Biomaterials.25:3559-68. 2004.

36. Salerno A, Iannace S, Netti PA. Open-Pore Biodegradable Foams Prepared via Gas Foaming and Microparticulate Templating. Macromolecular Bioscience.8:655-64. 2008.

37. Gualandi C, White LJ, Chen L, Gross RA, Shakesheff KM, Howdle SM, et al. Scaffold for tissue engineering fabricated by non-isothermal supercritical carbon dioxide foaming of a highly crystalline polyester. Acta Biomaterialia.6:130-6. 2010.

38. Mathieu LM, Montjovent MO, Bourban PE, Pioletti DP, Manson JA. Bioresorbable composites prepared by supercritical fluid foaming. J Biomed Mater Res A.75:89-97. 2005.

39. Tsivintzelis I, Pavlidou E, Panayiotou C. Biodegradable polymer foams prepared with supercritical CO2-ethanol mixtures as blowing agents. The Journal of Supercritical Fluids.42:265-72. 2007.

40. White LJ, Hutter V, Tai H, Howdle SM, Shakesheff KM. The effect of processing variables on morphological and mechanical properties of supercritical CO(2) foamed scaffolds for tissue engineering. Acta Biomater. 2011.

41. Tsivintzelis I, Pavlidou E, Panayiotou C. Porous scaffolds prepared by phase inversion using supercritical CO2 as antisolvent: I. Poly(l-lactic acid). The Journal of Supercritical Fluids.40:317-22. 2007.

42. Reverchon E, Cardea S, Rappo ES. Production of loaded PMMA structures using the supercritical CO2 phase inversion process. Journal of Membrane Science.273:97-105. 2006.

43. Duarte ARC, Mano JF, Reis RL. Dexamethasone-loaded scaffolds prepared by supercritical-assisted phase inversion. Acta Biomaterialia.5:2054-62. 2009.

44. Duarte ARC, Mano JF, Reis RL. The role of organic solvent on the preparation of chitosan scaffolds by supercritical assisted phase inversion. The Journal of Supercritical Fluids.In Press, Corrected Proof.

45. Butler R, Davies CM, Cooper AI. Emulsion Templating Using High Internal Phase Supercritical Fluid Emulsions. Advanced Materials.13:1459-63. 2001.

46. Levit N, Tepper G. Supercritical CO2-assisted electrospinning. The Journal of Supercritical Fluids.31:329-33. 2004.

47. Liu J, Shen Z, Lee S-H, Marquez M, McHugh MA. Electrospinning in compressed carbon dioxide: Hollow or open-cell fiber formation with a single nozzle configuration. The Journal of Supercritical Fluids.53:142-50. 2010.

48. Ayodeji O, Graham E, Kniss D, Lannutti J, Tomasko D. Carbon dioxide impregnation of electrospun polycaprolactone fibers. The Journal of Supercritical Fluids.41:173-8. 2007.

49. Li D, Xia Y. Electrospinning of Nanofibers: Reinventing the Wheel? Advanced Materials.16:1151-70. 2004.

50. Toyokawa N, Fujioka H, Kokubu T, Nagura I, Inui A, Sakata R, et al. Electrospun Synthetic Polymer Scaffold for Cartilage Repair Without Cultured Cells in an Animal Model. Arthroscopy : the journal of arthroscopic & related surgery : official publication of the Arthroscopy Association of North America and the International Arthroscopy Association.26:375-83. 2010.

51. Shields KJ, Beckman MJ, Bowlin GL, Wayne JS. Mechanical properties and cellular proliferation of electrospun collagen type II. Tissue Eng.10:1510-7. 2004.

52. Thorvaldsson A, Stenhamre H, Gatenholm P, Walkenström P. Electrospinning of Highly Porous Scaffolds for Cartilage Regeneration. Biomacromolecules.9:1044-9. 2008.

53. Ekaputra AK, Zhou Y, Cool SM, Hutmacher DW. Composite electrospun scaffolds for engineering tubular bone grafts. Tissue Eng Part A.15:3779-88. 2009.

54. Ramachandran K, Gouma PI. Electrospinning for bone tissue engineering. Recent Pat Nanotechnol.2:1-7. 2008.

55. Ishii O, Shin M, Sueda T, Vacanti JP. In vitro tissue engineering of a cardiac graft using a degradable scaffold with an extracellular matrix-like topography. J Thorac Cardiovasc Surg.130:1358-63. 2005.

56. Lim SH, Mao H-Q. Electrospun scaffolds for stem cell engineering. Advanced Drug Delivery Reviews.61:1084-96. 2009.

57. McCullen SD, Stevens DR, Roberts WA, Clarke LI, Bernacki SH, Gorga RE, et al. Characterization of electrospun nanocomposite scaffolds and biocompatibility with adipose-derived human mesenchymal stem cells. Int J Nanomedicine.2:253-63. 2007.

58. Rubenstein DA, Venkitachalam SM, Zamfir D, Wang F, Lu H, Frame MD, et al. In vitro biocompatibility of sheath-core cellulose-acetate-based electrospun scaffolds towards endothelial cells and platelets. J Biomater Sci Polym Ed.21:1713-36. 2010.

59. Drury JL, Mooney DJ. Hydrogels for tissue engineering: scaffold design variables and applications. Biomaterials.24:4337-51. 2003.

60. Tsioptsias C, Panayiotou C. Foaming of chitin hydrogels processed by supercritical carbon dioxide. The Journal of Supercritical Fluids.47:302-8. 2008.

61. Tsioptsias C, Paraskevopoulos MK, Christofilos D, Andrieux P, Panayiotou C. Polymeric hydrogels and supercritical fluids: The mechanism of hydrogel foaming. Polymer.52:2819-26. 2011.

62. Annabi N, Mithieux SM, Weiss AS, Dehghani F. The fabrication of elastin-based hydrogels using high pressure CO2. Biomaterials.30:1-7. 2009.

63. Hile DD, Amirpour ML, Akgerman A, Pishko MV. Active growth factor delivery from poly(D,L-lactide-co-glycolide) foams prepared in supercritical CO(2). J Control Release.66:177-85. 2000.

64. Velasco D, Benito L, Fernández-Gutiérrez M, San Román J, Elvira C. Preparation in supercritical CO2 of porous poly(methyl methacrylate)-poly(l-lactic acid) (PMMA-PLA) scaffolds incorporating ibuprofen. The Journal of Supercritical Fluids.54:335-41. 2010.

65. Duarte ARC, Mano JF, Reis RL. Preparation of chitosan scaffolds loaded with dexamethasone for tissue engineering applications using supercritical fluid technology. European Polymer Journal.45:141-8. 2009.

66. Kanczler JM, Ginty PJ, Barry JJA, Clarke NMP, Howdle SM, Shakesheff KM, et al. The effect of mesenchymal populations and vascular endothelial growth factor delivered from biodegradable polymer scaffolds on bone formation. Biomaterials.29:1892-900. 2008.

67. Santo VE, Duarte ARC, Gomes ME, Mano JF, Reis RL. Hybrid 3D structure of poly(d,l-lactic acid) loaded with chitosan/chondroitin sulfate nanoparticles to be used as carriers for biomacromolecules in tissue engineering. The Journal of Supercritical Fluids.54:320-7. 2010.

68. Nie H, Lee LY, Tong H, Wang CH. PLGA/chitosan composites from a combination of spray drying and supercritical fluid foaming techniques: new carriers for DNA delivery. J Control Release.129:207-14. 2008.

69. Ginty PJ, Howard D, Rose FRAJ, Whitaker MJ, Barry JJA, Tighe P, et al. Mammalian cell survival and processing in supercritical CO2. Proceedings of the National Academy of Sciences.103:7426-31. 2006.

70. Ginty PJ, Howard D, Upton CE, Barry JJA, Rose FRAJ, Shakesheff KM, et al. A supercritical CO2 injection system for the production of polymer/mammalian cell composites. The Journal of Supercritical Fluids.43:535-41. 2008.

71. Singh M, Sandhu B, Scurto A, Berkland C, Detamore MS. Microsphere-based scaffolds for cartilage tissue engineering: Using subcritical CO2 as a sintering agent. Acta Biomaterialia.6:137-43. 2010.

72. Oh SH, Park IK, Kim JM, Lee JH. In vitro and in vivo characteristics of PCL scaffolds with pore size gradient fabricated by a centrifugation method. Biomaterials.28:1664-71. 2007.

73. Dehghani F, Annabi N. Engineering porous scaffolds using gas-based techniques. Current Opinion in Biotechnology.In Press, Corrected Proof.

74. Tai H, Mather ML, Howard D, Wang W, White LJ, Crowe JA, et al. Control of pore size and structure of tissue engineering scaffolds produced by supercritical fluid processing. Eur Cell Mater.14:64-77. 2007.

75. Reverchon E, Cardea S, Rapuano C. A new supercritical fluid-based process to produce scaffolds for tissue replacement. The Journal of Supercritical Fluids.45:365-73. 2008.

76. Baker KC, Bellair R, Manitiu M, Herkowitz HN, Kannan RM. Structure and mechanical properties of supercritical carbon dioxide processed porous resorbable polymer constructs. Journal of the Mechanical Behavior of Biomedical Materials.2:620-6. 2009.

77. Goel SK, Beckman EJ. Generation of microcellular polymeric foams using supercritical carbon dioxide. I: Effect of pressure and temperature on nucleation. Polymer Engineering & Science.34:1137-47. 1994.

78. Jaklenec A, Hinckfuss A, Bilgen B, Ciombor DM, Aaron R, Mathiowitz E. Sequential release of bioactive IGF-I and TGF-β1 from PLGA microsphere-based scaffolds. Biomaterials.29:1518-25. 2008.

79. Kucharska M, Walenko K, Butruk B, Brynk T, Heljak M, Ciach T. Fabrication and characterization of chitosan microspheres agglomerated scaffolds for bone tissue engineering. Materials Letters.64:1059-62. 2010.

80. Jiang T, Nukavarapu SP, Deng M, Jabbarzadeh E, Kofron MD, Doty SB, et al. Chitosan–poly(lactide-co-glycolide) microsphere-based scaffolds for bone tissue engineering: In vitro degradation and in vivo bone regeneration studies. Acta Biomaterialia.6:3457-70. 2010.

81. Jiang T, Nukavarapu SP, Deng M, Jabbarzadeh E, Kofron MD, Doty SB, et al. Chitosan-poly(lactide-co-glycolide) microsphere-based scaffolds for bone tissue engineering: in vitro degradation and in vivo bone regeneration studies. Acta Biomater.6:3457-70. 2010.

82. Borden M, Attawia M, Khan Y, Laurencin CT. Tissue engineered microsphere-based matrices for bone repair:: design and evaluation. Biomaterials.23:551-9. 2002.

83. Berkland C, Kim K, Pack DW. PLG Microsphere Size Controls Drug Release Rate Through Several Competing Factors. Pharmaceutical Research.20:1055-62. 2003.

84. Lu JM, Wang X, Marin-Muller C, Wang H, Lin PH, Yao Q, et al. Current advances in research and clinical applications of PLGA-based nanotechnology. Expert Rev Mol Diagn.9:325-41. 2009.

85. Tracy MA, Ward KL, Firouzabadian L, Wang Y, Dong N, Qian R, et al. Factors affecting the degradation rate of poly(lactide-co-glycolide) microspheres in vivo and in vitro. Biomaterials.20:1057-62. 1999.

86. Wu L, Ding J. In vitro degradation of three-dimensional porous poly(D,L-lactide-co-glycolide) scaffolds for tissue engineering. Biomaterials.25:5821-30. 2004.

87. Brown JL, Nair LS, Laurencin CT. Solvent/non-solvent sintering: a novel route to create porous microsphere scaffolds for tissue regeneration. J Biomed Mater Res B Appl Biomater.86:396-406. 2008.

88. Singh M, Morris CP, Ellis RJ, Detamore MS, Berkland C. Microsphere-based seamless scaffolds containing macroscopic gradients of encapsulated factors for tissue engineering. Tissue Eng Part C Methods.14:299-309. 2008.

89. Singh M, Sandhu B, Scurto A, Berkland C, Detamore MS. Microsphere-based scaffolds for cartilage tissue engineering: using subcritical CO(2) as a sintering agent. Acta Biomater.6:137-43. 2010.

90. Berkland C, Kim K, Pack DW. Fabrication of PLG microspheres with precisely controlled and monodisperse size distributions. J Control Release.73:59-74. 2001.

91. Mohan N, Dormer NH, Caldwell KL, Key VH, Berkland CJ, Detamore MS. Continuous Gradients of Material Composition and Growth Factors for Effective Regeneration of the Osteochondral Interface. Tissue Eng Part A. 2011.

92. Fan H, Zhang C, Li J, Bi L, Qin L, Wu H, et al. Gelatin microspheres containing TGF-beta3 enhance the chondrogenesis of mesenchymal stem cells in modified pellet culture. Biomacromolecules.9:927-34. 2008.

93. Heng BC, Cao T, Lee EH. Directing stem cell differentiation into the chondrogenic lineage in vitro. Stem Cells.22:1152-67. 2004.

94. Knippenberg M, Helder MN, Zandieh Doulabi B, Wuisman PI, Klein-Nulend J. Osteogenesis versus chondrogenesis by BMP-2 and BMP-7 in adipose stem cells. Biochem Biophys Res Commun.342:902-8. 2006.

95. Sun J, Yu YC, Gu ZY, Gu L, Bi W. [Effect of BMP-2 on osteogenesis of bone mesenchymal stem cells in rats]. Shanghai Kou Qiang Yi Xue.20:352-7. 2011.

96. Edwards CA, O'Brien WD, Jr. Modified assay for determination of hydroxyproline in a tissue hydrolyzate. Clin Chim Acta.104:161-7. 1980.

97. Boyan BD, Schwartz Z, Bonewald LF, Swain LD. Localization of 1,25-(OH)2D3-responsive alkaline phosphatase in osteoblast-like cells (ROS 17/2.8, MG 63, and MC 3T3) and growth cartilage cells in culture. J Biol Chem.264:11879-86. 1989.

98. Livak KJ, Schmittgen TD. Analysis of relative gene expression data using real-time quantitative PCR and the 2(-Delta Delta C(T)) Method. Methods.25:402-8. 2001.

99. Singh M, Detamore MS. Stress relaxation behavior of mandibular condylar cartilage under high-strain compression. J Biomech Eng.131:061008. 2009.

100. Agrawal CM, Athanasiou KA. Technique to control pH in vicinity of biodegrading PLA-PGA implants. J Biomed Mater Res.38:105-14. 1997.

101. Wang L, Sheshareddy K, Weiss ML, Detamore MS. Effect of initial seeding density on human umbilical cord mesenchymal stromal cells for fibrocartilage tissue engineering. Tissue Eng Part A.15:1009-17. 2009.

102. Jaiswal N, Haynesworth SE, Caplan AI, Bruder SP. Osteogenic differentiation of purified, culture-expanded human mesenchymal stem cells in vitro. J Cell Biochem.64:295-312. 1997.

103. Nuttelman CR, Tripodi MC, Anseth KS. Synthetic hydrogel niches that promote hMSC viability. Matrix Biol.24:208-18. 2005.

Appendix A

Table 1: Recent developments in $scCO_2$ gas foaming and phase inversion

References	Scaffold material	CO_2 process conditions	Scaffold fabrication method	Major Results	Applications
Salerno *et al.* (36)	PCL with micrometric NaCl particles	Soaking Pressure: 65 bar Soaking Temp: 70˚C Soaking Time: 3 hrs	Gas foaming and micro particulate templating.	1. Microparticle concentration gradients of NaCl were used to prepare open-pore foams with spatial gradients of porosity and pore size. 2.Varying the microparticle concentration resulted in the control of porosity (in the range 78-93%) and pore size from 90 to 10 µm.	This technique can be tailored to design the micro-architecture of open pore foams with respect to desired applications.
Gualandi *et al.* (37)	Co-polymer of ω-pentadecalactone (PDL) and ε-caprolactone(CL), poly (PDL-	Soaking Pressure: 230 bar Soaking Temp: 90˚C Soaking Time: 20min dP/dt=4 bar/min dT/dt=0˚C/min, 0.15˚C/min, 0.23˚C/min and 0.27˚C/min	$scCO_2$ gas foaming.	1. Cooling rate of 0.23˚C min^{-1} showed best results with pore diameter of 255 µm and 70% porosity. 2. Short soaking time (1 min) led to a non-porous core with a porous shell, t_{soak} of 10 min led to pore size of 155 µm and 57% porosity. Increasing t_{soak} to 20 min decreased pore size to 110 µm. 3. Better average pore size and interconnectivity was obtained by decreasing the rate of depressurization.	(PDL-CL) can find applications in cartilage tissue engineering.

	CL)			4. The compressive modulus values obtained were in the same range as that of articular cartilage.	
Mathieu *et al.*(38)	PLA with hydroxyapatite (HA) and β-tricalcium phosphate (β-TCP)	Soaking Pressure: 100 to 250 bar Soaking Temp: 195˚C Soaking Time: 10 min dP/dt=2 to 15 bar/s dT/dt=3 to 7˚C/s	$scCO_2$ gas foaming.	1. Composite cellular structures obtained had a heterogeneous architecture with more closed pores. 2. A 5% filler content is the maximum possible to obtain foams with adequate microstructure (especially pore size and interconnections) 3. Addition of HA resulted in more heterogeneous foams than with β-TCP. Ceramic particles got distributed in the pore walls of the composite foams, thereby providing an efficient reinforcement of the matrix. 4. Filled foams had modulus of up to 250 MPa with average pore size from 200-400 μm and porosities between 78 and 92%.	Applications in bone tissue engineering.
Tsivintzelis *et al.* (39)	PCL	Soaking Pressure: 123-205 bar Soaking Temp: 35-45˚C	$scCO_2$ gas foaming with ethanol as blowing agent.	1. Crystalline polymers can undergo $scCO_2$ foaming by addition of small amounts of organic solvents. 2. Pure CO_2 as blowing agent resulted in a heterogeneous structure with regions of different pore sizes and densities. In contrast, constructs prepared using CO_2 and ethanol exhibited more uniform cell structures. This also resulted in larger pore formation. 3. All samples had dense unfoamed skin usually seen with gas foaming technique.	--

Tsivintzelis *et al.* (41)	PLLA	Saturation Pressure: 100,165,230 bar Saturation Temp=45˚C Saturation time: 2.5 h dP/dt: 1 bar/min Solvent: Dichloromethane	Phase inversion using $scCO_2$ antisolvent.	1. Pore size decreased with pressure variation from 100-230 bar. Decrease in temperature (or increase in pressure) increases density and solvent power of CO_2. 2. Lesser initial polymer concentration leads to larger pore formation.	--
Reverchon *et al.* (42)	PMMA	Saturation Pressure:200 bar Saturation Temp: 45˚C Saturation Time: 45 min Solvent: DMSO and acetone	Phase inversion using $scCO_2$ antisolvent.	1. Increase in polymer concentration leads to decrease in pore size in both solvents. 2. L-L demixing is the controlling mechanism. 3. Pore interconnectivity observed in acetone but closed pores in DMSO. 4.Increase in pressure from 150 to 250 bar causes decrease in pore diameter from 15 to 7 µm. Increase in temperature from 35-65˚C increases pore size from 8 to 12 µm.	PMMA loaded with an antibiotic, amoxicillin for drug delivery applications.
Duarte *et al.* (43)	Starch and Poly(L-lactic acid) (SPLA)	Saturation Pressure: 200 bar Saturation Temp: 55˚C Saturation time: 45 min dP/dt: 5 g/min	Phase inversion using $scCO_2$ antisolvent.	1. Polymer matrices are bicontinuous surfaces that have micro and macropores; highly interconnected pores. 2. Porosity up to 66% and pore size of macropores is 200 µm, micropores is 20-50 µm 3. Up to 90% swelling and weight loss of about 25% observed after 21 days in solution.	SPLA loaded with dexamethasone to be used in bone tissue engineering applications.

Duarte *et al.* (44)	Chitosan	Saturation Pressure: 15 MPa Saturation Temp: 60°C Saturation time: 45 min dP/dt: 5 g/min	Phase inversion using $scCO_2$ antisolvent.	Formic acid as a solvent resulted in 29% porosity and average pore size 62 µm; acetic acid: 47% porosity and 110 µm pore size; HFIP: 90% porosity and 600 µm pore size.	Bone & Cartilage regeneration

Appendix B

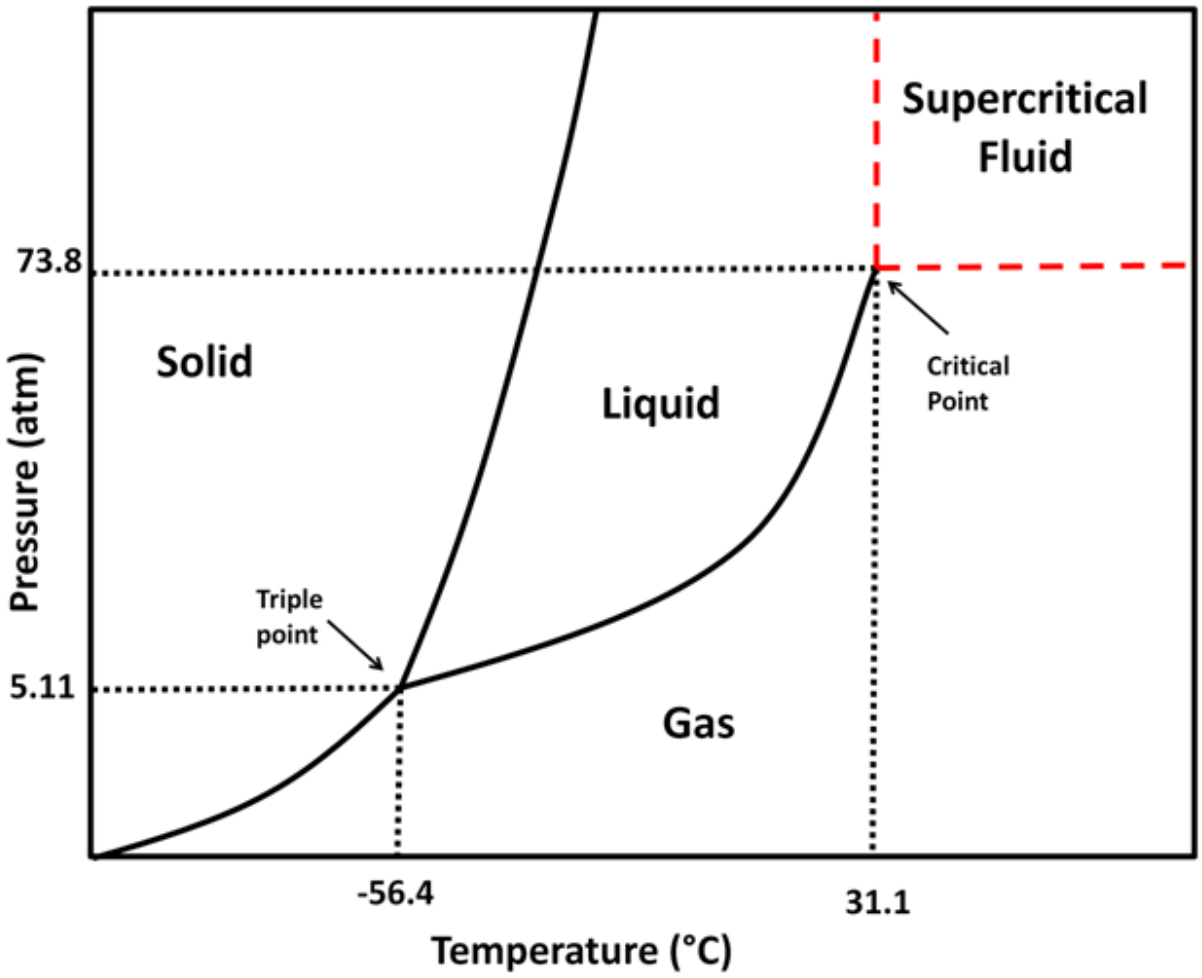

Figure 1: Schematic of carbon dioxide (CO_2) pressure-temperature phase diagram.

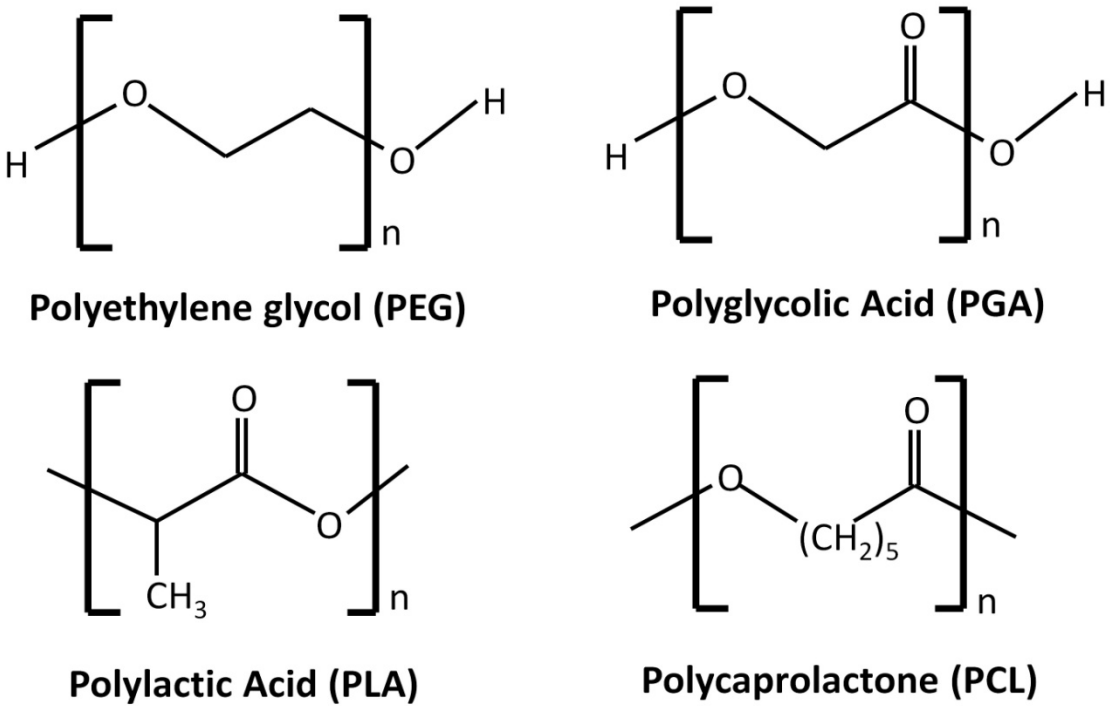

Figure 2: Chemical structures of some common polymers.

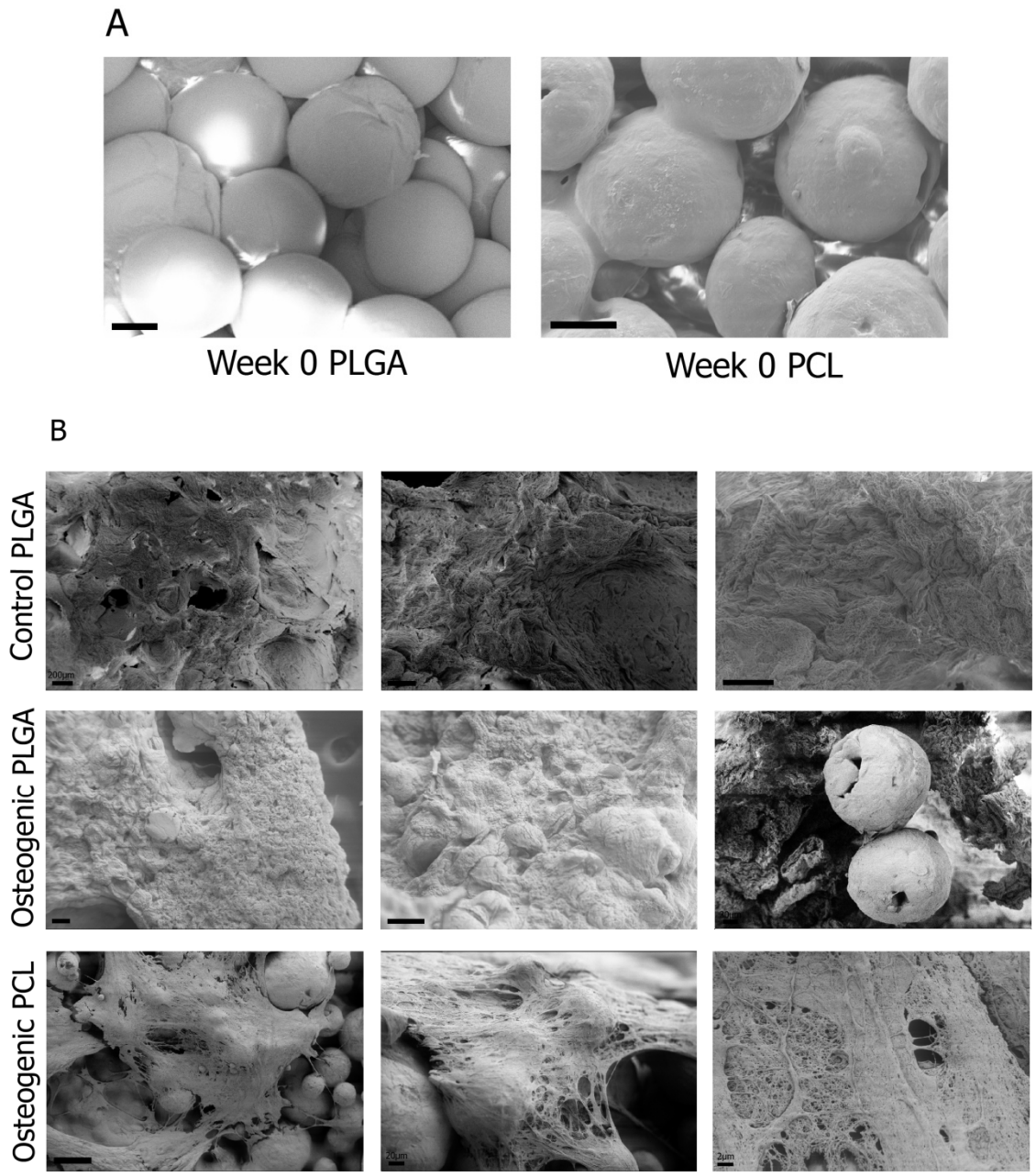

Figure 3: Selected scanning electron microscopy (SEM) images of week 0 (A) and week 6 (B) samples. Scaffolds were fabricated using PLGA and PCL microspheres at customized processing conditions for sintering (CO_2 exposure at 25 bar for 1 h at 25ºC followed by depressurization at a rate of 0.101 psi s^{-1} for PLGA; 45 bar for 4 hrs at 45 ºC followed by depressurization at a rate of 0.2 psi s^{-1} for PCL). Comparable degrees of sintering were observed at week 0, and microsphere shape was better preserved in the PCL constructs by week 6. Chondrogenic PLGA scaffolds have not been shown as they could not withstand SEM processing. Scale bars = 100 μm unless shown otherwise.

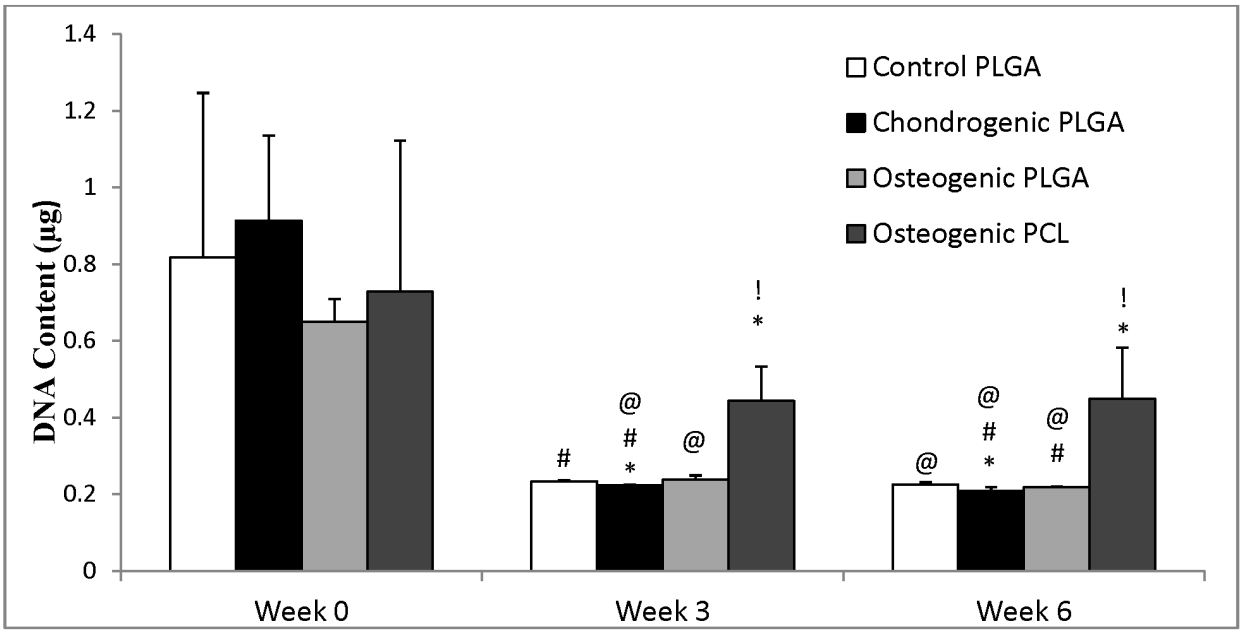

Figure 4: DNA content for all groups. All the three PLGA groups had statistically significant decrease in cell number by week 6 compared to the week 0 Control group. Only Osteogenic PCL group had similar cell number throughout 6 weeks. It had significantly higher cell number over the control group at all times. Values are reported as mean ± standard deviation, n = 4. Statistically significant difference @ = from the week 0 value (Control PLGA) ($p < 0.05$), # = from its value at the previous time point ($p < 0.05$), and * = from the control (Control PLGA) at that time point ($p < 0.05$), and ! = between the two osteogenic groups at that time point ($p < 0.05$).

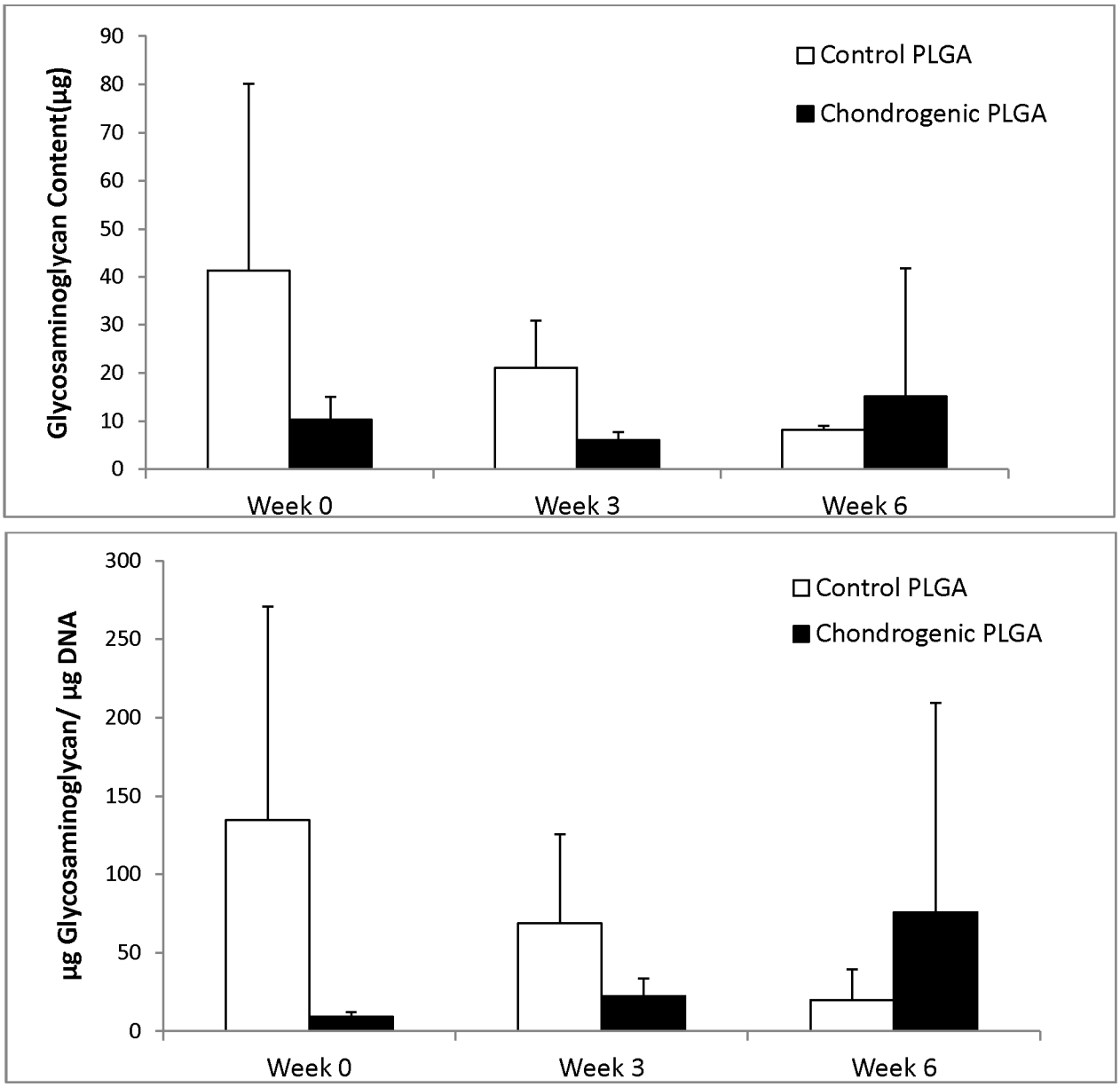

Figure 5: Glycosaminoglycan (GAG) content for the chondrogenic groups. Significant changes in the GAG content were not observed for the Control PLGA and Chondrogenic PLGA groups. Values are reported as mean ± standard deviation, n = 4.

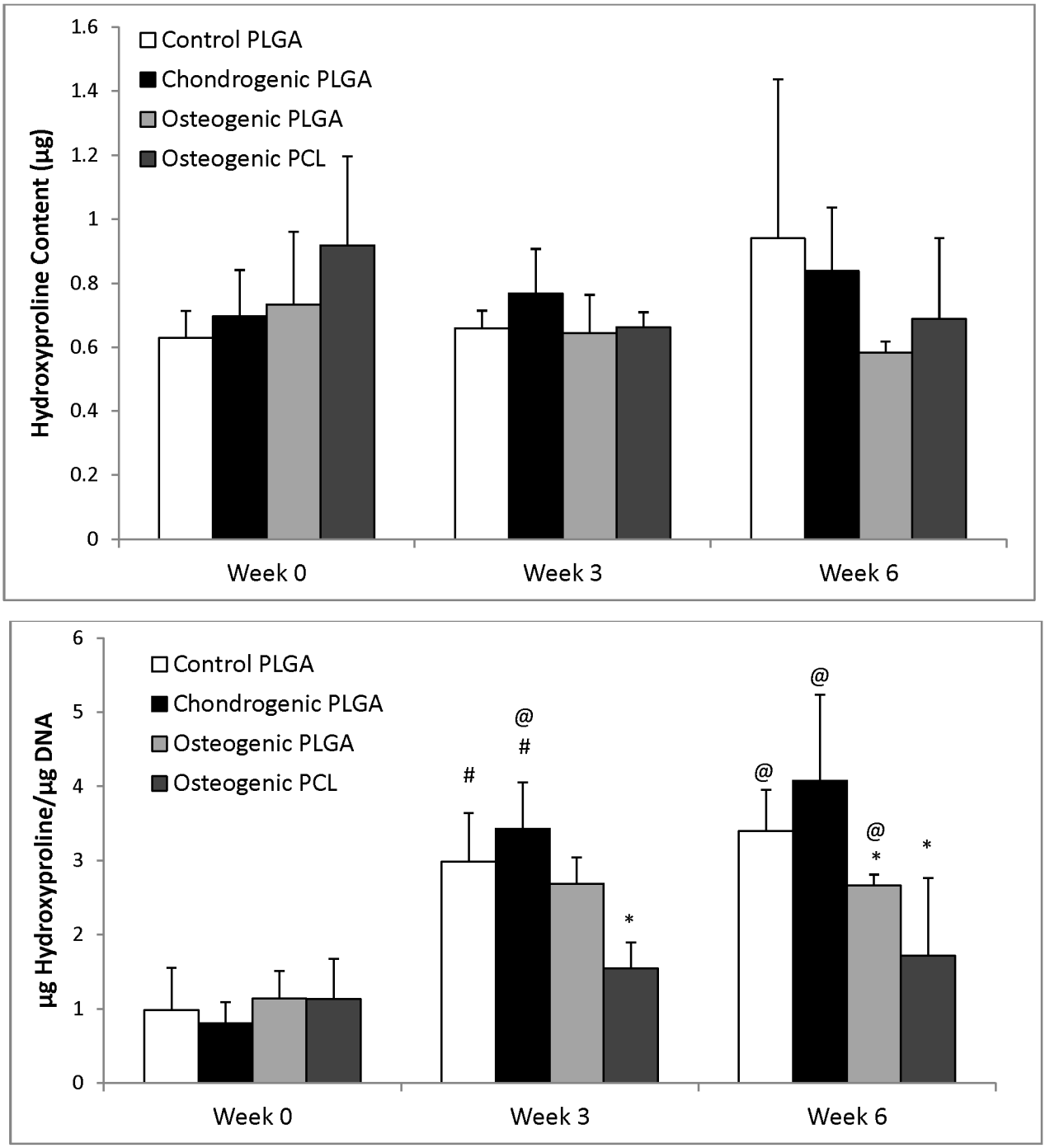

Figure 6: Hydroxyproline (HYP) content for all groups. (A) Statistically significant differences in HYP content were not observed in any group. (B) All groups had statistically significant increases in HYP/DNA content at week 3 and 6. The Chondrogenic PLGA constructs had significantly higher production relative to control at week 0 when compared to all other groups.

Values are reported as mean ± standard deviation, n = 4. Statistically significant difference @ = from the week 0 value (Control PLGA) ($p < 0.05$), # = from its value at the previous time point ($p < 0.05$), * = from the control (Control PLGA) at that time point ($p < 0.05$), and ! = between the two osteogenic groups at that time point ($p < 0.05$).

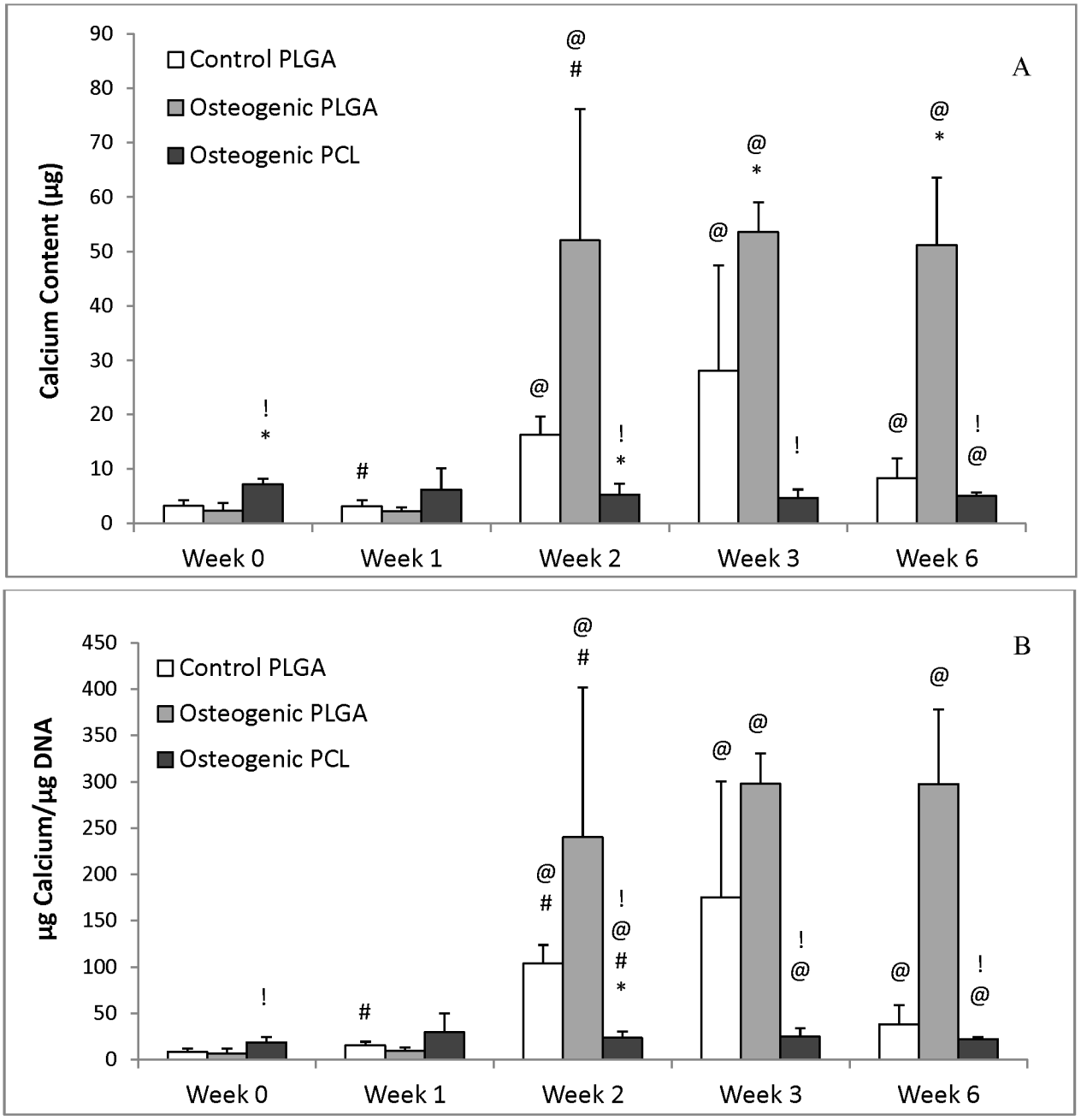

Figure 7: Calcium content for the osteogenic groups. (A) Most groups had statistically significant increases in calcium content from week 0 to week 6, but only the Osteogenic PLGA constructs had significantly higher production relative to the control at 6 weeks. Notably, this value was at least 6 times higher than any other group at the end of the culture. At 6 weeks, the Osteogenic PCL group showed a decrease in calcium content when compared to the Control group. (B) Osteogenic PLGA constructs produced more Calcium/DNA than Control and PCL groups at week 6. An increasing Calcium/ DNA content trend was observed for Control and Osteogenic PCL groups till week 3. Week 6 showed decreased values for both groups. Values

are reported as mean ± standard deviation, n = 4. Statistically significant difference @ = from the week 0 value (Control PLGA) ($p < 0.05$), # = from its value at the previous time point ($p < 0.05$), * = from the control (Control PLGA) at that time point ($p < 0.05$) and ! = between the two osteogenic groups at that time point ($p < 0.05$).

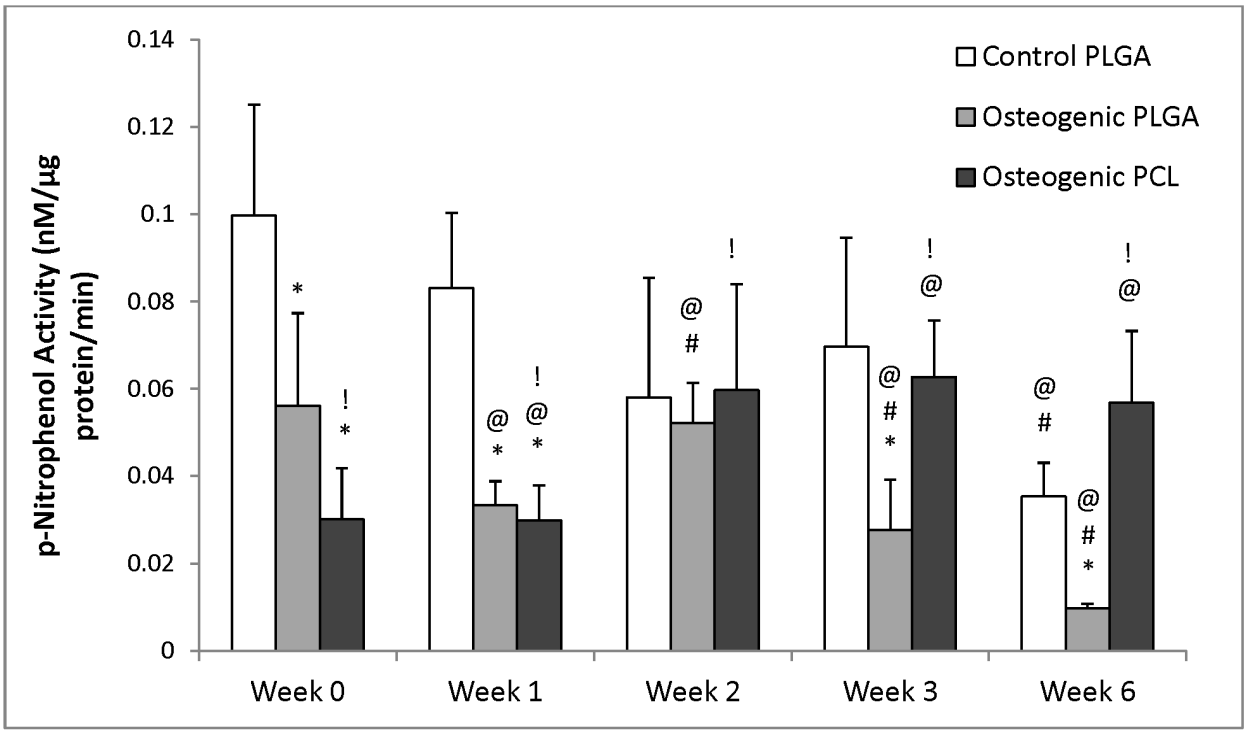

Figure 8: Alkaline Phosphatase activity of the osteogenic groups. Alkaline phosphatase activity for all constructs showed a varying trend throughout the 6 weeks. Control PLGA group showed a decreasing ALP content while Osteogenic PCL had an increasing ALP content at the end of week 6. Osteogenic PLGA constructs had an increasing ALP activity till week 3 after which they decreased. Values are reported as mean ± standard deviation, n = 4. Statistically significant difference @ = from the week 0 value (Control PLGA) ($p < 0.05$), # = from its value at the previous time point ($p < 0.05$), * = from the control (Control PLGA) at that time point ($p < 0.05$) and ! = between the two osteogenic groups at that time point ($p < 0.05$).

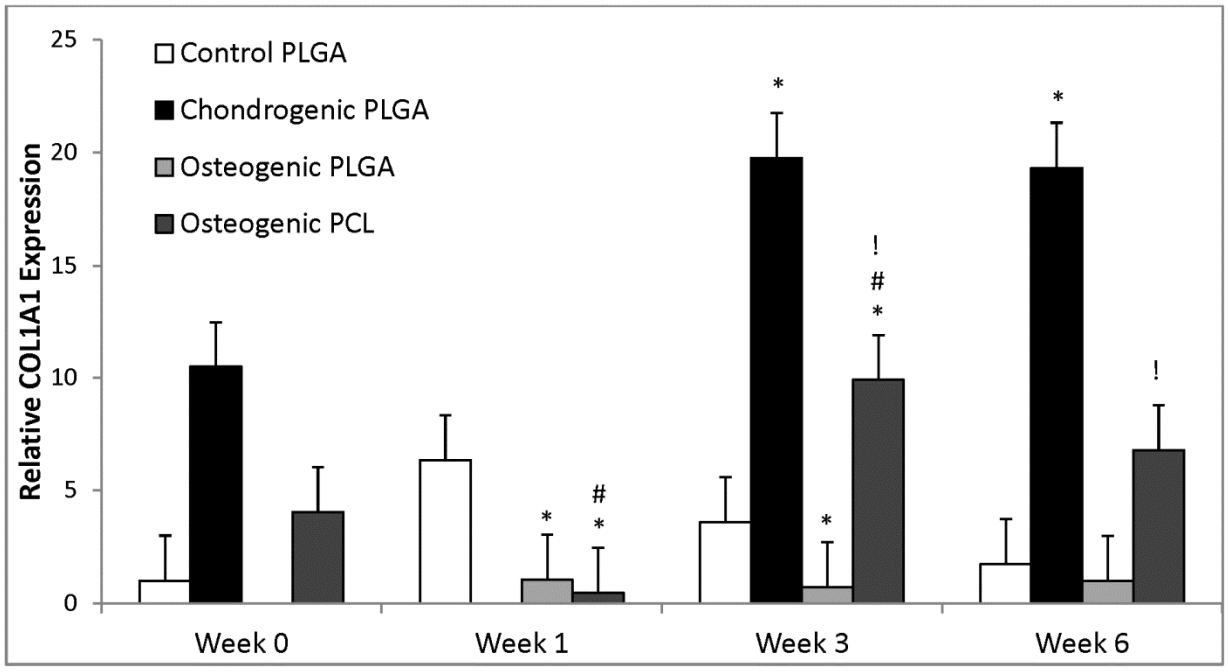

Figure 9: Relative COL1A1 expression. Statistically significant changes in COL1A1 expression were observed. Increased expression over week 0 value was seen in week 3 Osteogenic PCL constructs. Osteogenic PLGA constructs showed no significant changes over the weeks. Calibrator group: Week 0 Control PLGA group. Endogenous group: GAPDH. Values are reported as mean ± standard deviation, n= 4. Statistically significant change of expression * = from the control PLGA group at that time point, # = from its value at the previous time point ($p < 0.05$) and ! = between the two osteogenic groups at that time point ($p < 0.05$).

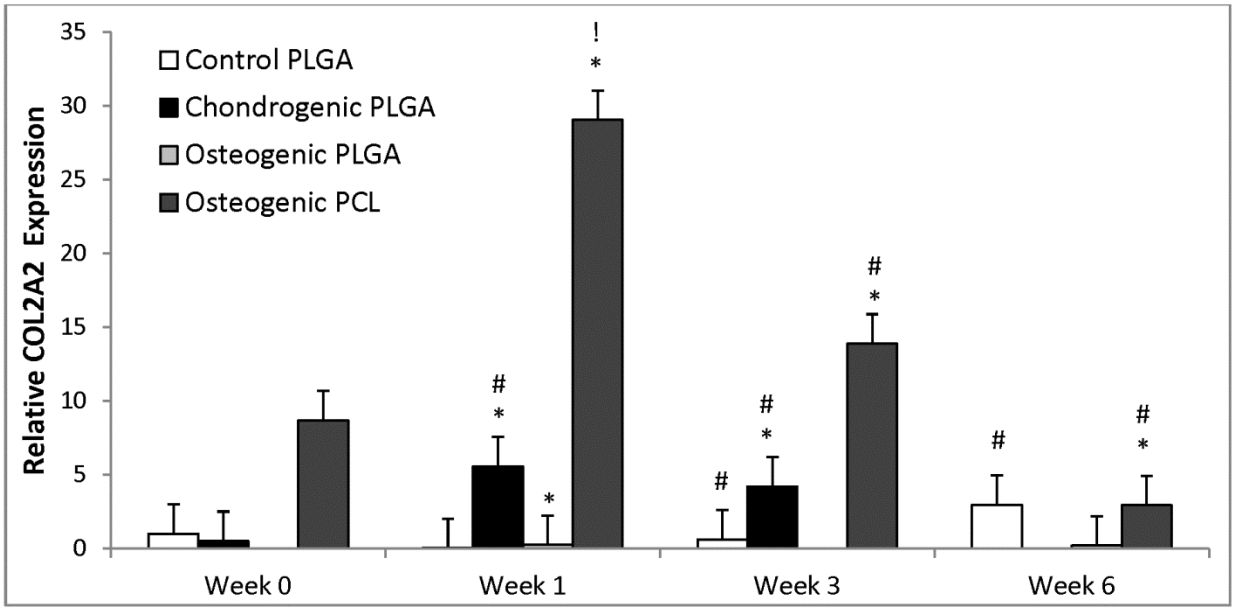

Figure 10: Relative COL2A2 expression. Statistically significant increase in COL2A2 expression at week 1 and 3 was observed for the chondrogenic PLGA group over its week 0 value. Increase in expression was observed the control PLGA group as well at week 6 over the previous time point was observed only in week 6 Osteogenic groups. There was a decrease in COL2A2 expression in osteogenic groups towards the end of 6 weeks. Calibrator group: Week 0 Control PLGA group. Endogenous group: GAPDH. Values are reported as mean ± standard deviation, n=4. Statistically significant change of expression * = from the control PLGA group at that time point, # = from its value at the previous time point ($p < 0.05$) and ! = between the two osteogenic groups at that time point ($p < 0.05$).

.

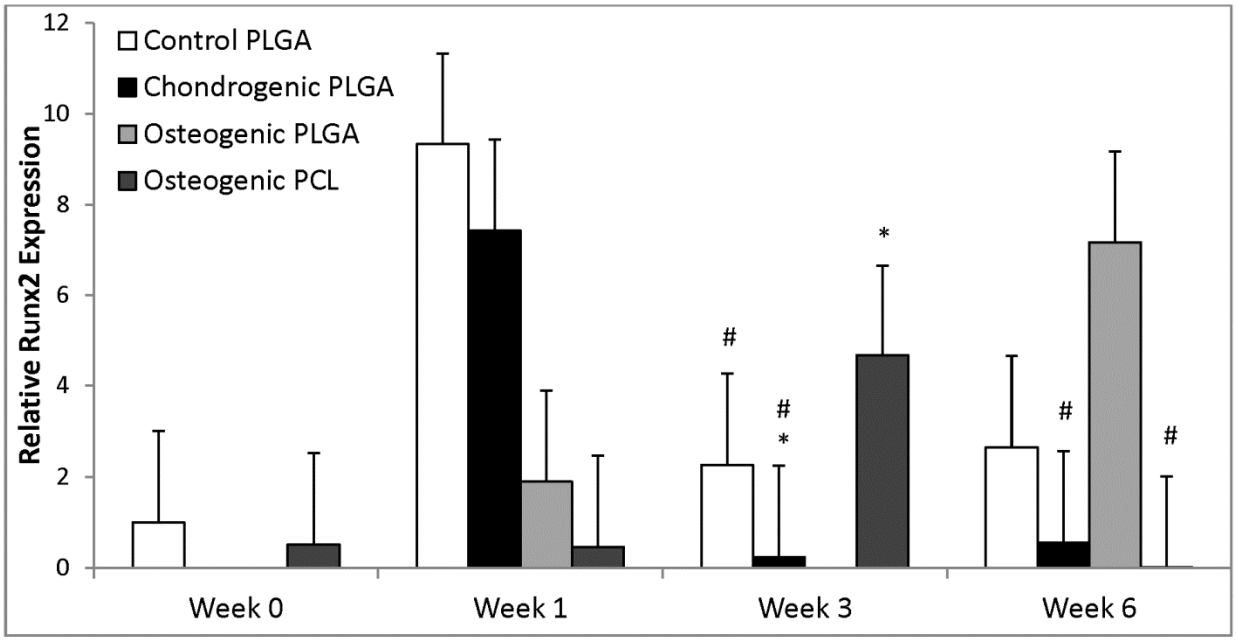

Figure 11: Relative Runx2 expression. Statistically significant changes were observed in the Osteogenic PLGA group. Runx2 expression was found to increase in PLGA group near week 6. Expression increased in the Osteogenic PCL group at week 3 while control PLGA group had a decrease in expression at the end of week 6. Calibrator group: Week 0 Control PLGA group. Endogenous group: GAPDH. Values are reported as mean ± standard deviation, n=4. Statistically significant change of expression * = from the control PLGA group at that time point, # = from its value at the previous time point ($p < 0.05$) and ! = between the two osteogenic groups at that time point ($p < 0.05$).

.

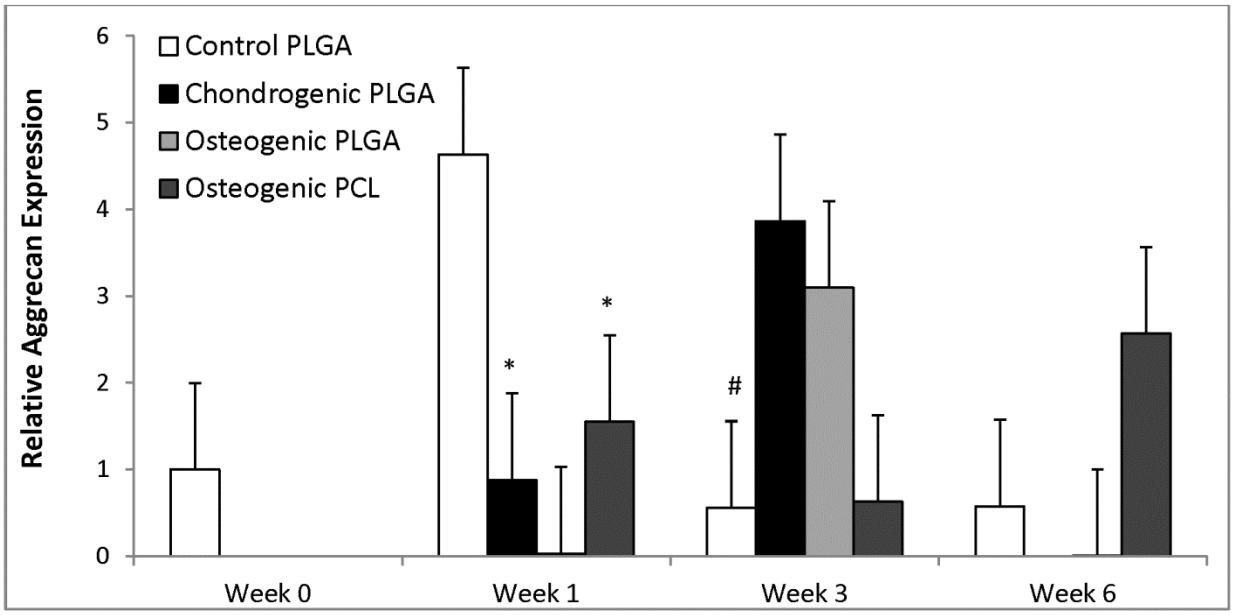

Figure 12: Relative Aggrecan expression. Relative aggrecan expression had no statistically significant changes during the 6 weeks except for the control PLGA group. Increased expression was seen in the Chondrogenic group and the two osteogenic groups. Calibrator group: Week 0 Control PLGA group. Endogenous group: GAPDH. Values are reported as mean ± standard deviation, n= 4. Statistically significant change of expression * = from the control PLGA group at that time point, # = from its value at the previous time point ($p< 0.05$) and ! = between the two osteogenic groups at that time point ($p < 0.05$).

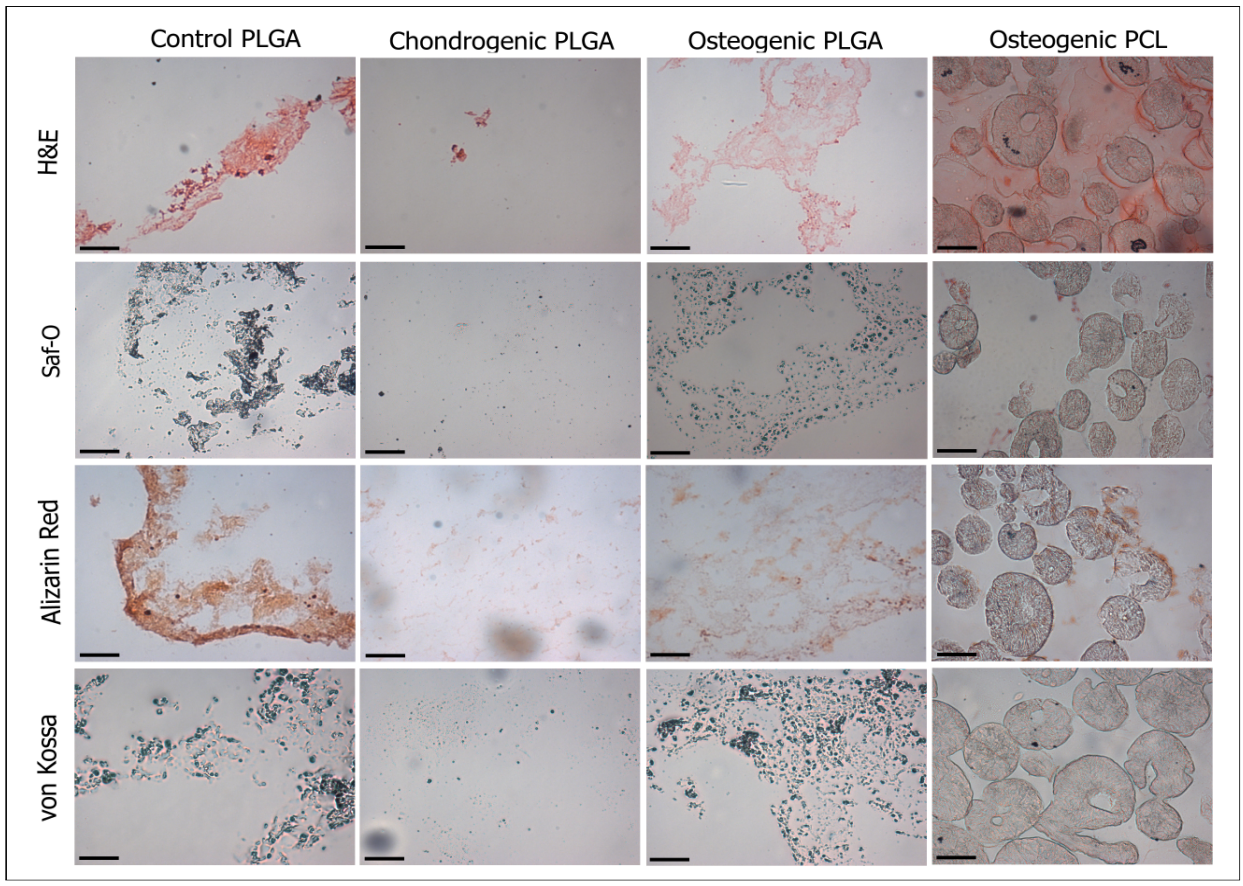

Figure 13: Histological staining of constructs at week 3. At week 3, Control PLGA and Osteogenic PLGA constructs showed calcium and calcium phosphate deposits mainly on the periphery of the scaffolds. GAG staining was very low with positive staining mainly in Osteogenic PCL constructs. Cell nuclei were seen in all constructs except Chondrogenic PLGA with H&E staining. Scale bars = 100 μm.

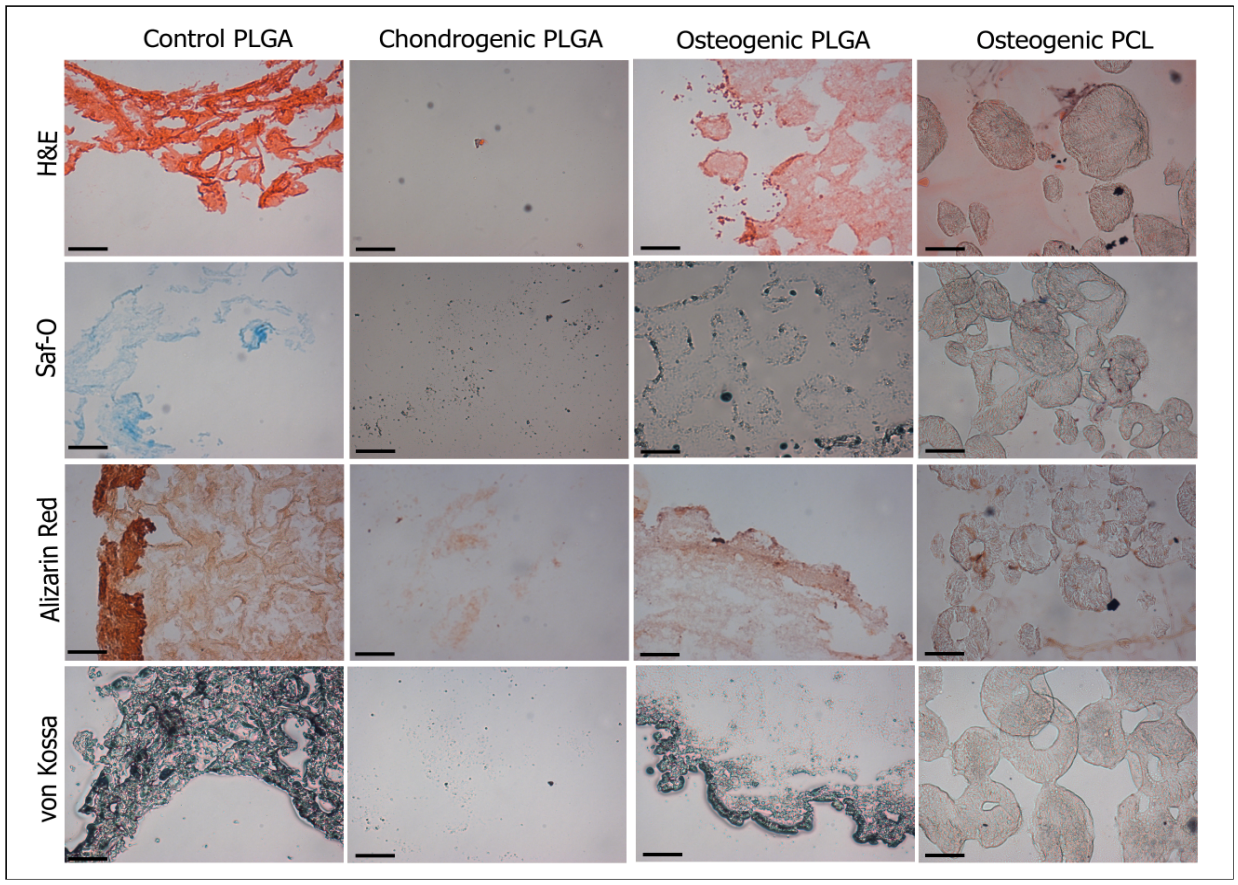

Figure 14: Histological staining of constructs at week 6. Histological staining of constructs at week 6 revealed calcium depositions in the periphery of scaffolds for Control and Osteogenic PLGA groups. Reduced numbers of cell nuclei were observed in all groups except Osteogenic PLGA. Saf-O staining did not show a lot of GAG production. Scale bars = 100 µm.

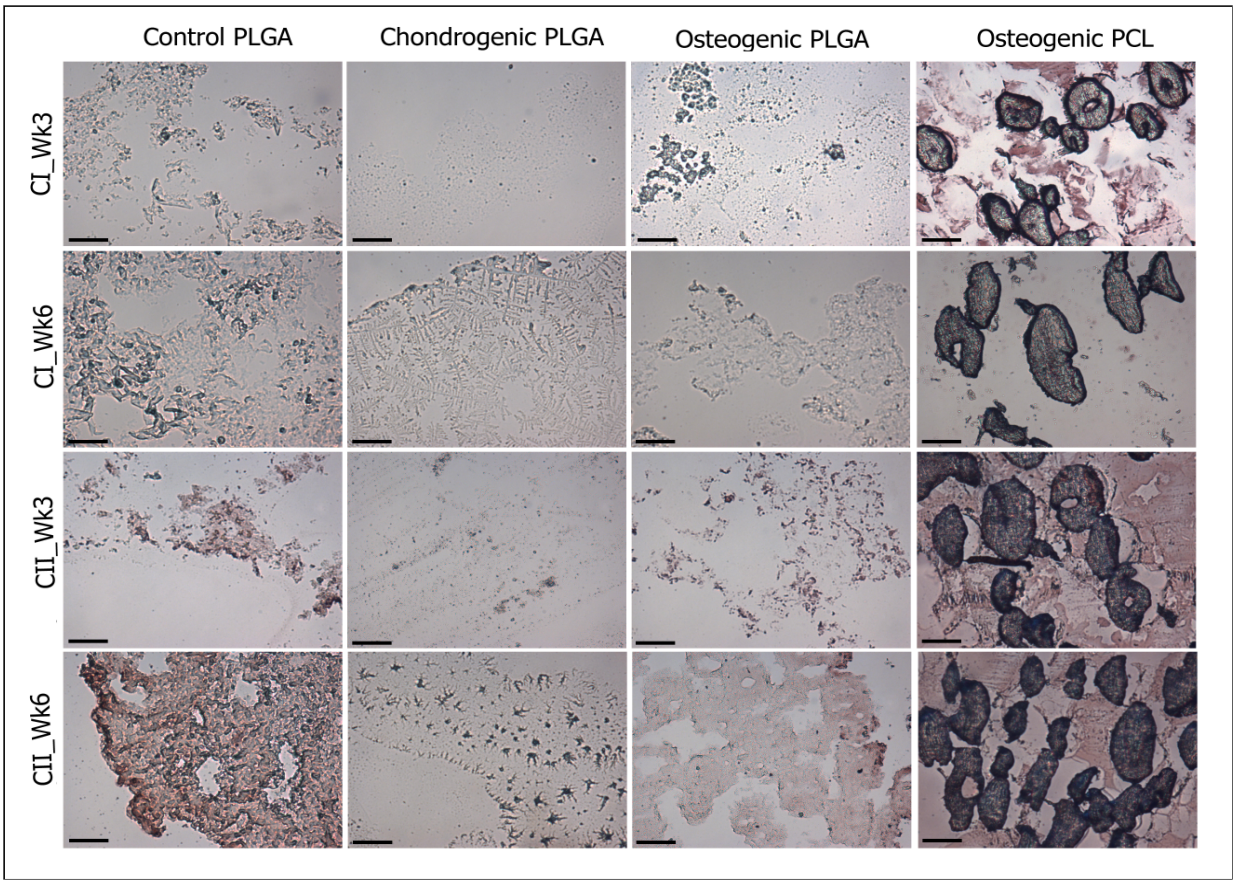

Figure 15: Immunohistochemical staining for types I and II collagen. By 3 weeks, positive immunostaining was observed for type I collagen with relatively more expression in Osteogenic PLGA and Control PLGA groups. Presence of type II collagen was seen mostly in Control PLGA group. By 6 weeks, both type I and type II collagen was seen in all groups with maximum staining in the control group followed by Osteogenic PLGA group. Scale bars = 100 µm.

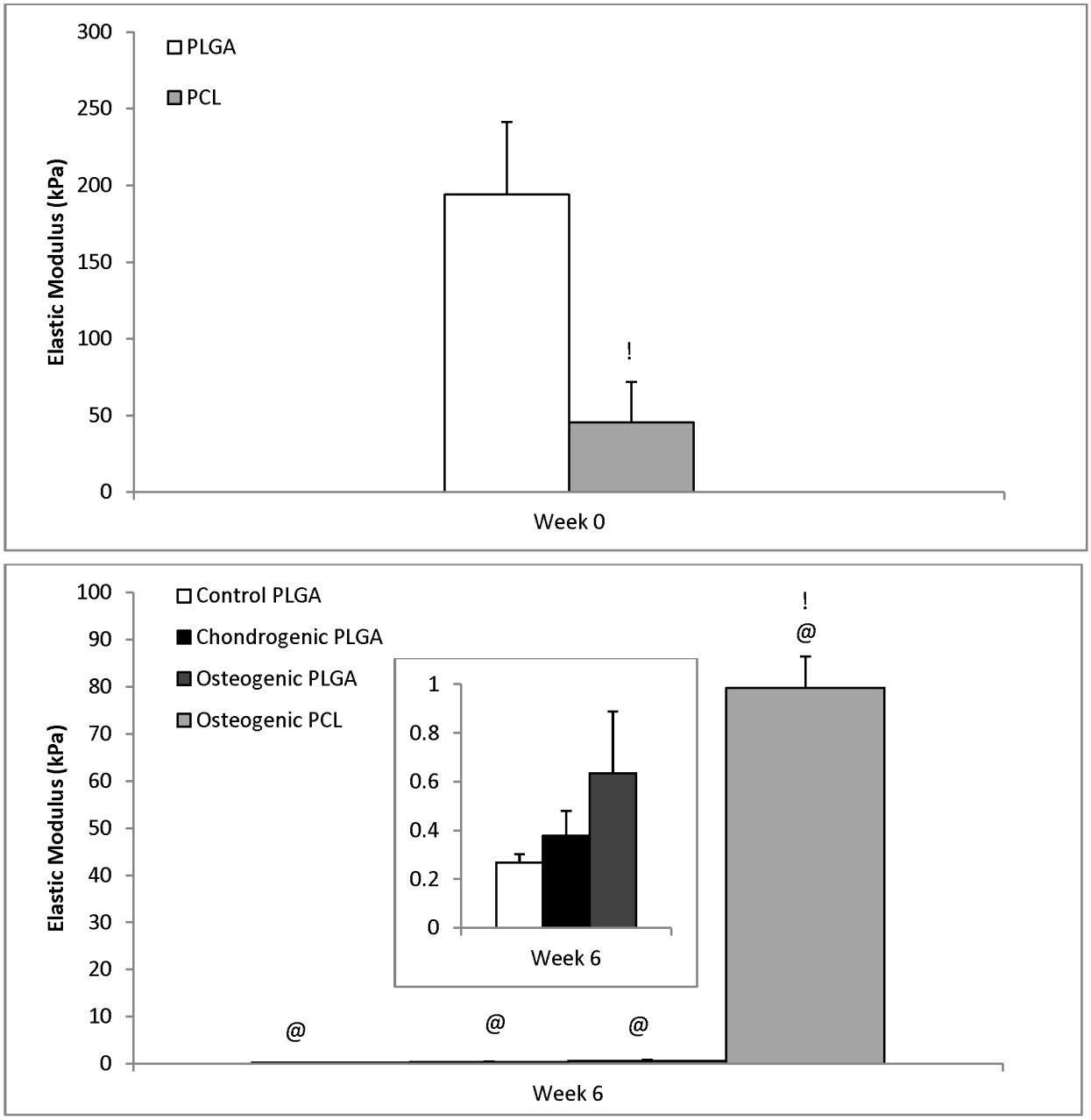

Figure 16: Elastic modulus (kPa) at week 0 (A) and week 6 (B). Elastic modulus at week 0 for both the groups PLGA and PCL were significantly different from one another. PLGA had a higher modulus at 193.98 ± 47.38 kPa while PCL had a modulus of 45.59 ± 26.29 kPa. Inset graph represents the three PLGA groups. At week 6, a statistically significant decrease in elastic modulus was observed for the three PLGA groups. Osteogenic PLGA group was statistically higher over the control at week 6. Osteogenic PCL on the other hand, increased in elastic modulus after 6 weeks in culture. Values are expressed as mean ± standard deviation, n = 5.

Statistically significant difference @ = from the week 0 Control PLGA value ($p < 0.05$), and ! = between the two osteogenic groups at that time point ($p < 0.05$).

Appendix C

Representative Stress-Strain curves for all groups at different time points

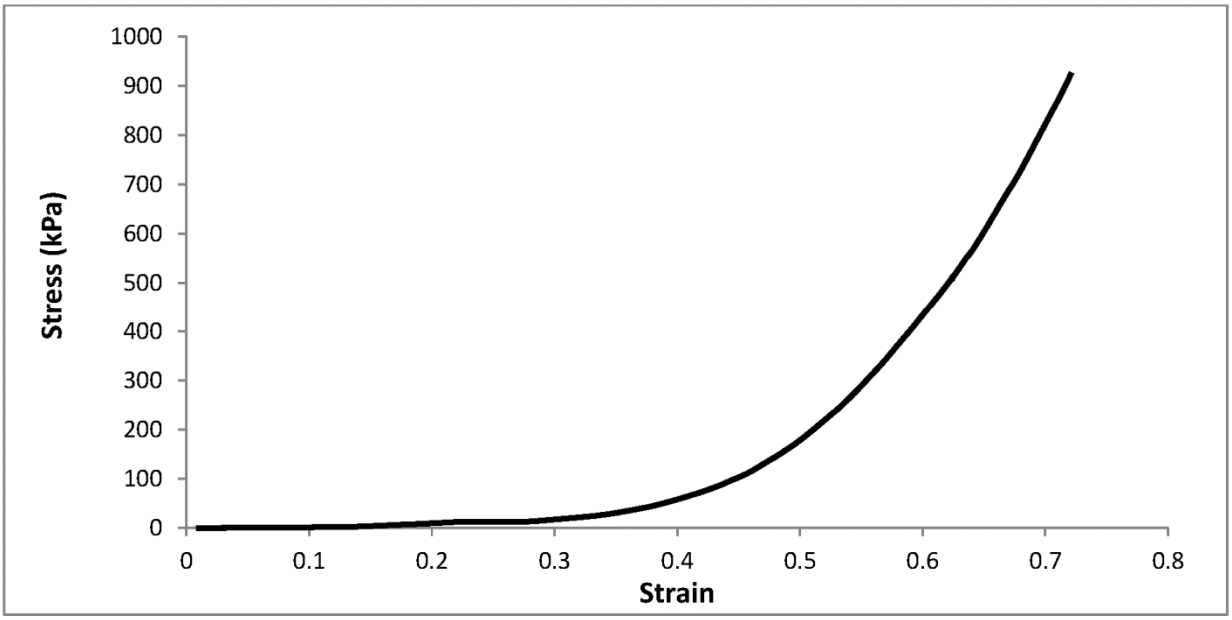

Figure 17 : Stress-Strain curve of week 0 Osteogenic PCL group from compression testing. Engineering stress values (kPa) are shown. Compressive modulus extracted from the initial linear region (up to 20% strain).

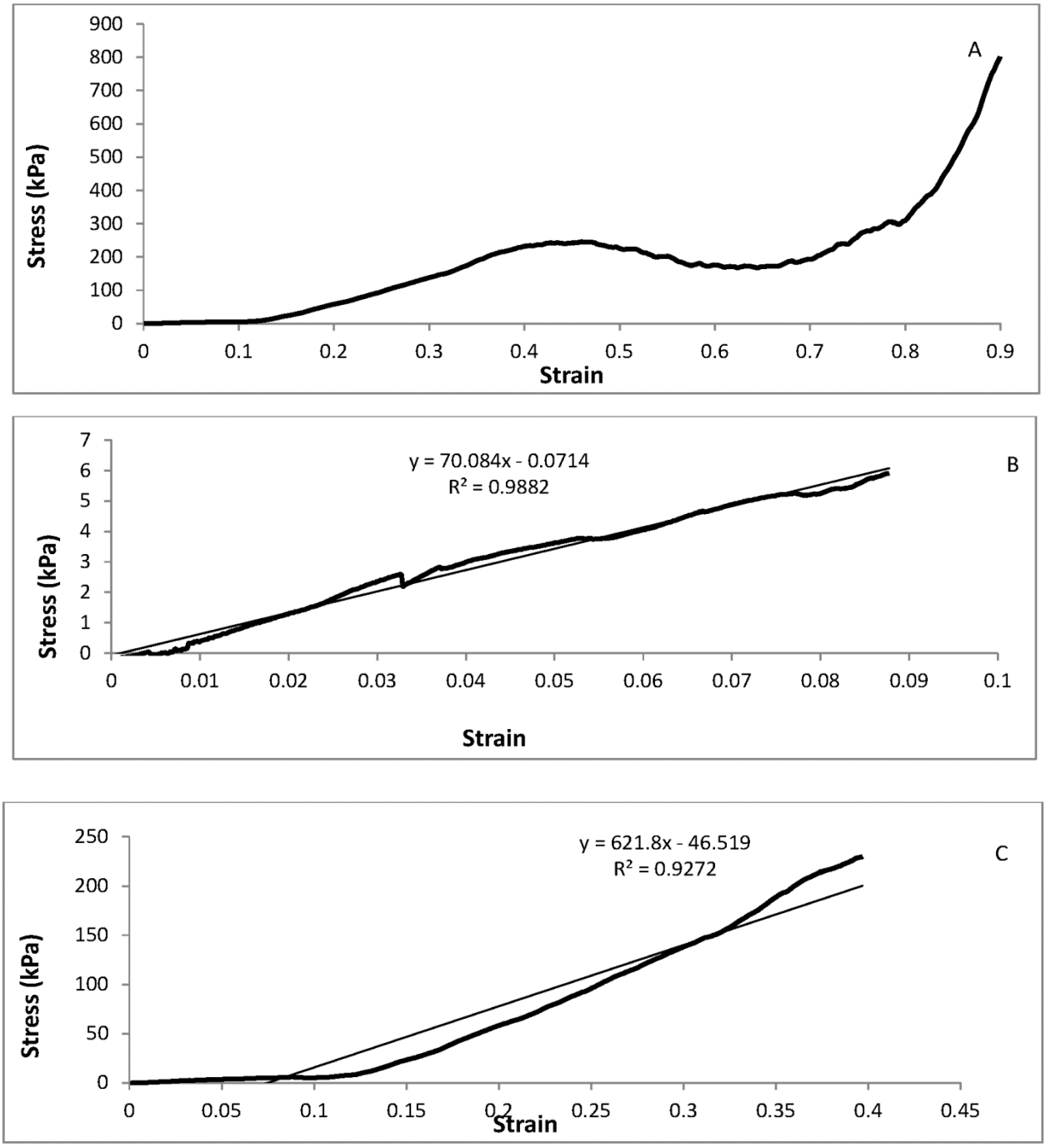

Figure 18: (A) Stress-Strain curve of week 6 Osteogenic PCL group from compression testing. Engineering stress values (kPa) are shown. (B) Compressive modulus extracted from the initial linear region (up to 10% strain). (C) Compressive modulus extracted from 0 to 40% strain.

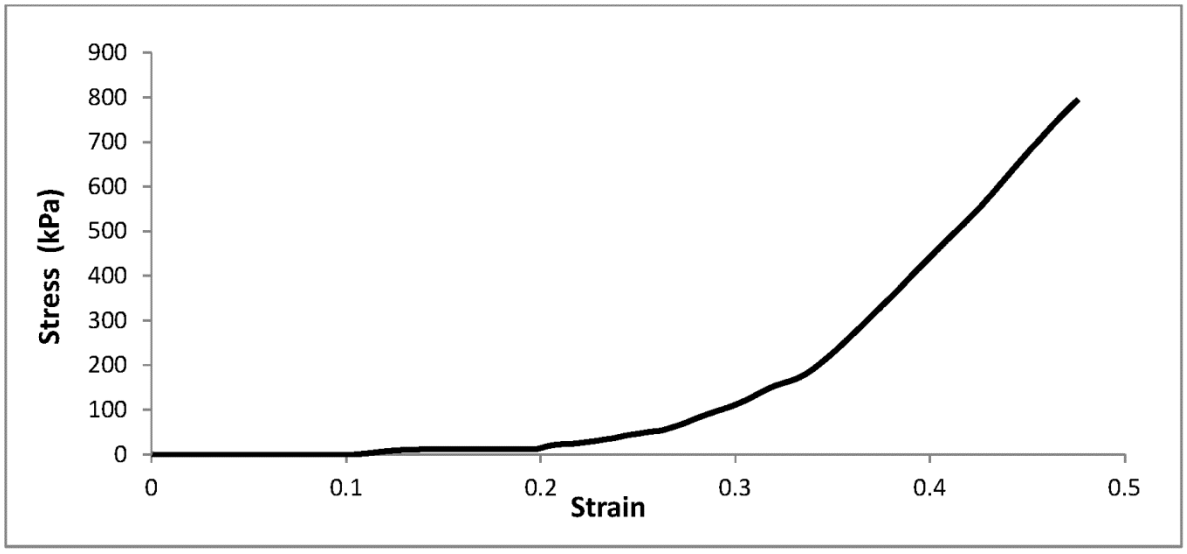

Figure 19: Stress-Strain curve of week 0 Control PLGA group from compression testing. Engineering stress values (kPa) are shown. Compressive modulus extracted from the initial linear region (up to 20% strain).

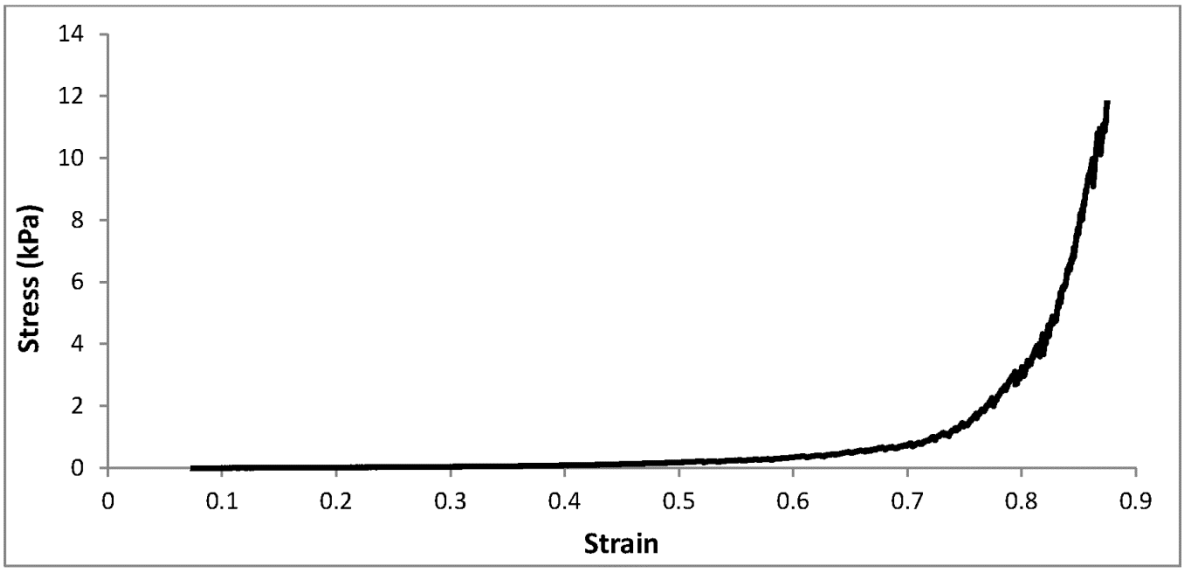

Figure 20: Stress-Strain curve of week 6 Control PLGA group from compression testing. Engineering stress values (kPa) are shown. Compressive modulus extracted from the initial linear region (up to 40% strain).

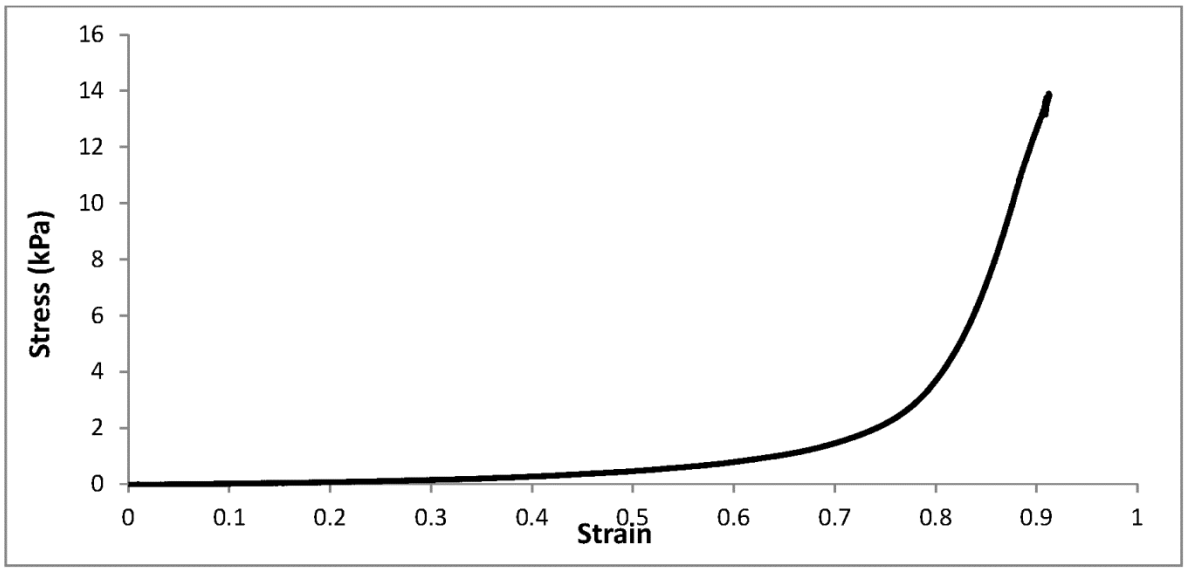

Figure 21: Stress-Strain curve of week 6 Osteogenic PLGA group from compression testing. Engineering stress values (kPa) are shown. Compressive modulus extracted from the initial linear region (up to 40% strain).

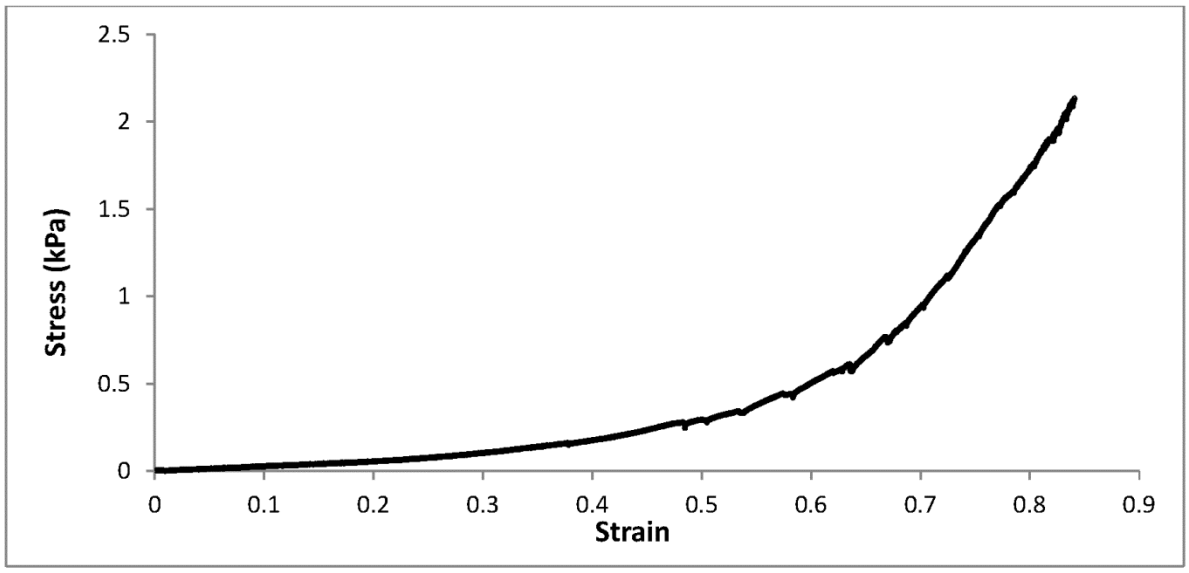

Figure 22: Stress-Strain curve of week 6 Chondrogenic PLGA group from compression testing. Engineering stress values (kPa) are shown. Compressive modulus extracted from the initial linear region (up to 40% strain).

Appendix D

Table 2: CO_2 sintering parameters for PCL

Pressure	Temperature	Exposure time	Depressurization time	Result
25 bar, 37 bar, 40 bar, 60 bar, 200 bar	Vessel temp: 25 ºC	1 hr	1 hr	Microspheres did not fuse at all.
25 bar, 200 bar	Vessel temp: 25 ºC	1 hr	Overnight	Microspheres did not fuse at all.
200 bar	Vessel temp: 25 ºC; CO_2 temp inside pump: 30 ºC, 35 ºC, 40 ºC	1 hr	1 hr	Microspheres did not fuse at all.
40 bar	Vessel temp: 25 ºC; 2 mL acetone added inside chamber.	1 hr	1 hr	Completely melted
40 bar	Vessel temp: 25 ºC; 0.5 mL acetone added inside chamber.	1 hr	1 hr	Completely melted.
25 bar	Vessel temp: 25 ºC; 0.5 mL acetone added inside chamber.	1 hr	1 hr	Partially melted.
No CO_2 exposure.	Placed in a 56 ºC water bath.	N/A	N/A	Fused partially.
No CO_2 exposure	Placed in a 60 ºC water bath.	N/A	N/A	Fused partially.
No CO_2 exposure	Placed in a 60 ºC oven.	N/A	N/A	Completely melted.
40 bar	Vessel temp: 30-35 ºC	1 hr	1 hr	Microspheres did not fuse at all.
72 bar	Vessel temp: 35 ºC	1 hr	1 hr	Microspheres did not fuse at all.

60 bar	Vessel temp: 40 ºC	1 hr	1 hr	Fused partially; scaffold disintegrated on touching.
47 bar, 50 bar	Vessel temp:42 ºC	1 hr	1 hr	Fused partially; scaffold disintegrated on touching.
45 bar	45 ºC	1 hr, 1hr 15 min, 2 hrs, 2 hrs 30 min	1 hr	Fused partially; scaffold disintegrated on touching.
45 bar	45 ºC	4 hr 15 min	1 hr	Melted completely.
45 bar	45 ºC	4 hr	1 hr 30 min	Melted completely.
45 bar	45 ºC	4 hr	30 min	Fused partially; scaffold disintegrated on touching.
45 bar	45 ºC	4 hr	45 min	Fused completely with each other. Construct disintegrated after 1 day in PBS.
45 bar	45 ºC	4 hr	1 hr	Microspheres completely fused with each other. Construct retained its integrity after 1 week in PBS at 37 ºC.